Geothermal Integrated System for Multi Generation

Omer Kalaf

Submitted to the
Institute of Graduate Studies and Research
in partial fulfillment of the requirements for the degree of

Master of Science
in
Mechanical Engineering

Eastern Mediterranean University
December 2016
Gazimağusa, North Cyprus

Approval of the Institute of Graduate Studies and Research

Prof. Dr. Mustafa Tümer
Director

I certify that this thesis satisfies the requirements as a thesis for the degree of Master of Science in Mechanical Engineering.

Assoc. Prof. Dr. Hasan Hacışevki
Chair, Department of Mechanical Engineering

We certify that we have read this thesis and that in our opinion it is fully adequate in scope and quality as a thesis for the degree of Master of Science in Mechanical Engineering.

Asst. Prof. Dr. Murat Özdenefe
Supervisor

Examining Committee

1. Prof. Dr. Fuat Egelioğlu

2. Assoc. Prof. Dr. Hasan Hacışevki

3. Asst. Prof. Dr. Murat Özdenefe

ABSTRACT

In this study, integrated, geothermal energy based system for multigeneration application with four useful outputs (electric power, heating, cooling, and hydrogen), which comprises from a Rankine Cycle (RC) for electrical power generation & for hot water recovery, and double effect absorption cooling cycle for cooling production, is proposed. The proposed system is investigated in detail. In order to determine the associated energies and irreversibilities in the system, the system components are investigated energetically and exergetically. The energy and exergy efficiencies of the RC are found to be 12.67% and 16.21%, respectively. Parametric studies are also performed to observe the effects of different parameters such as turbine inlet pressure, temperature and reference environment temperature on the exergy values. The energy and exergy COPs of the double effect absorption cooling system are found to be 1.437 and 0.3371, respectively. Exergy destruction is calculated for all the components, and it is found that maximum destruction occurred in RC high pressure turbine with 4021 kW and minimum destruction occurred in the condenser of double effect absorption cooling system (DEACS) which was 1.321kW.

Keywords: Multi generation, geothermal, energy, exergy, Rankine Cycle, absorption cooling.

ÖZ

Bu çalışmada, Rankine çevrimi kullanarak güç üretimi ile ısı geri kazanımı, çift etkili absorbsiyonlu soğutma sistemi kullanarak soğutma üretimi ve bunların yanında hidrojen üretimi sağlayan, jeotermal enerji tabanlı multijenerasyon uygulaması tasarlanmıştır. Tasarlanan sistem detaylı bir şekilde incelenmiştir. Sistem içerisinde bulunan her ekipmanm enerji ve ekserji incelemesi yapılmıştır. Rankine çevriminin enerji ve ekserji verimleri sırasıyla %12.67 ve % 16.21 olarak hesaplanmıştır. Bu çalışmada aynı zamanda, türbin giriş basıncı ve sıcaklığı ile referans çevre sıcaklığı gibi parametrelerin ekserji değerleri üzerindeki etkisini gözlemlemek için parametrik çalışma yapılmıştır. Çift etkili absorbsiyonlu soğutma sisteminin enerji ve ekserji COP'si sırasıyla 1.437 ve 0.3371 bulunmuştur. Sistemdeki tüm parçalarda gerçekleşen ekserji yıkımları hesaplanmış ve en büyük yıkımın 4021 kW ile Rankine çevrimi yüksek basınç türbininde, en küçük yıkımın ise 1.321 kW ile çift etkili absorbsiyonlu soğutma sisteminin kondanserinde gerçekleştiği bulunmuştur.

Anahtar Kelimeler: Multijenerasyon, jeotermal, enerji, ekserji, Rankine çevrimi, absorbsiyonlu soğutma

ACKNOWLEDGMENT

At first of all I express my thanks and appreciation to my supervisor Asst.Prof.Dr.Murat Özdenefe, for helping me during the period of search.

I would also to thank Asst. Prof. Dr. Tahir Abdul Hussain Ratlamwala for guidance to this study.

In the department, great thanks to Prof. Dr. Fuat Egelioğlu, Assoc. Prof. Dr. Hasan Hacışevki my Academic teachers.

By the end there are great thanks to my wife and my father and mother for all their supports in my life.

TABLE OF CONTENTS

LIST OF TABLES

LIST OF FIGURES

LIST OF SYMBOLS

BCHP	Building Cooling Heating and Power
CCHP	Combined Cooling, Heat and Power
CHP	Combined Heat and Power
COP	Coefficient of Performance
DEACS	Double Effect Absorption Cooling System
EES	Engineering Equation Solver
E_N	Energy
Ex	Exergy
$\dot{E}x$	Exergy Rate
HHV	High Heating Value
HRSG	Heat Recovery Steam Generator
HTF	High Temperature Fluid
IEA	International Energy Agency
LiBr-H_2O	Lithium bromide water
RC	Rankine Cycle
SOFC	Solid Oxide Fuel Cell
T	Temperature
T_0	Ambient Temperature
$\dot{M}_{H2}$	Hydrogen production
$\dot{Q}$	Heat
$\dot{W}$	Work

Subscripts

abs	Absorber

che	Condenser Heat Exchanger
cond	Condenser
evap	Evaporator
ex	Specific Exergy
he	Heat Exchanger
hhx	High Temperature Heat Exchanger
hpt	High Pressure Turbine
htg	High Temperature Generator
lhx	Low Temperature Heat Exchanger
lpt	Low Pressure Turbine
ltg	Low Temperature Generator
p	Pressure
v	Specific Volume
dest	Destruction
h_{H2}	Enthalpy of Hydrogen
$\dot{m}$	Mass Flow Rate
elec	Electrolyzer

Greek letters

$\in_U$	Utilization Factor
η_{th}	Thermal Efficiency
Ψ_{th}	Exergy Efficiency

Chapter 1

INTRODUCTION

1.1 Overview

Energy is key and important commodity to human well-being in modern times. On the surface of this planet there are seven billions of people and it is required to supply energy to cover their daily needs. In addition to that, the population growth and the booming economic development in the world leads to increased energy production (power, cooling, heating, etc.). Using fossil fuel, for producing power causes an increase in the pollutants in the air and this is a direct threat to human well being. In order to consume less fossil fuel and release less emission to air. It is crucial to use efficient systems for producing energy (power, cooling, heating etc.).

There are systems that use a single source of energy to produce electricity, heating, cooling etc. simultaneously which have higher efficiencies. These systems are called multigeneration systems and they are known as being very efficient. The concept of multi generation is shown in Figure 1.1

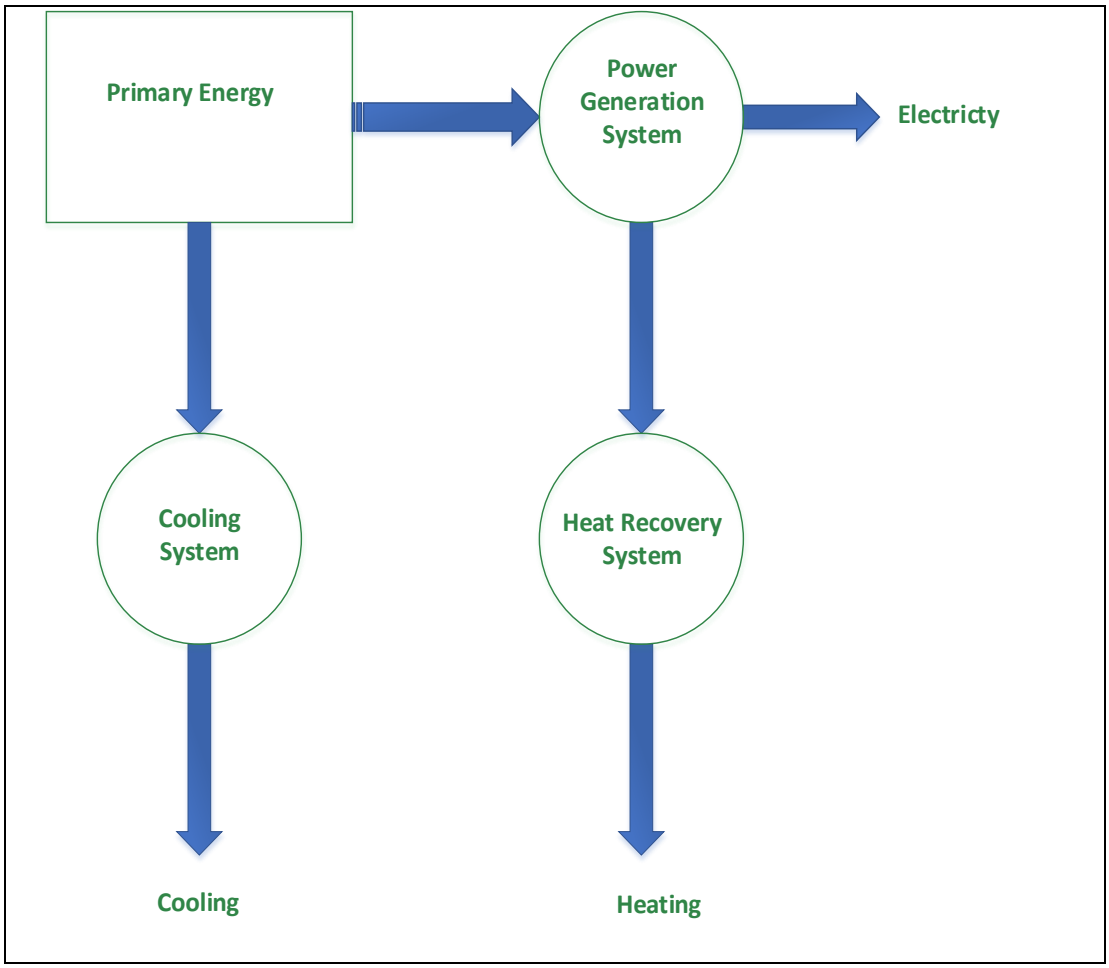

Figure 1.1: Depiction of multi generation system for three outputs (electricity, heating and cooling)

1.2 Importance of Energy

Energy demand is increasing all over the world. It has been predicted that global energy demand will increase by over one-third by 2035 and fossil fuels are still dominating the global energy [1]. The reasons for this increase are population growth, living standard and manufactory. While energy is needed for economic growth and sustainable development, energy consumption generates environmental and social impacts. The International Energy Agency (IEA) predicts that minimum 50% of total growth in global generation should be met by renewable energy sources during next 25 years; by this prediction the amount of emissions decreased because of less fossil fuel burning [2].

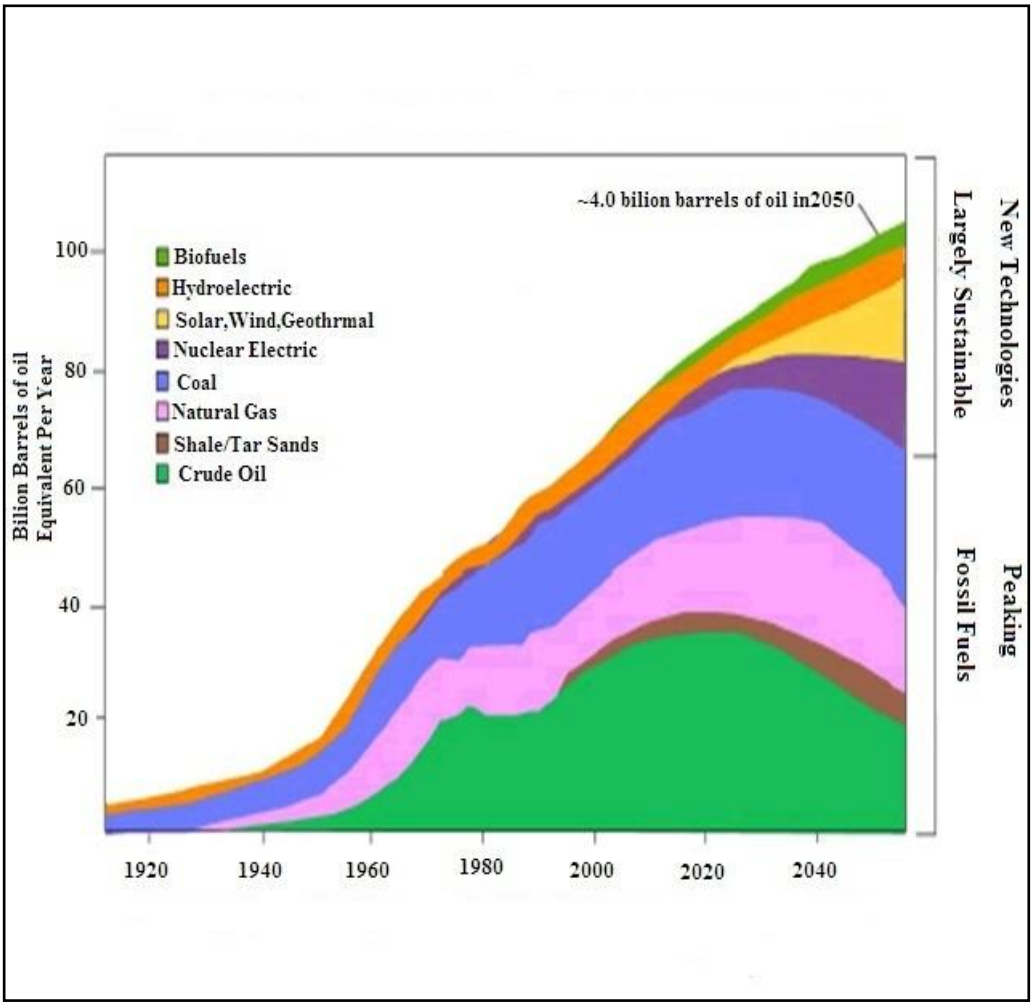

Figure 1.2: Energy use in the world [3]

Human of using power started long time ago, with discovery of fossil fuels such as coal, oil and gas, which caused a huge revolution in the industry. As a result of the growing demand for energy, the higher the ratio of greenhouse gases in the air, they think seriously about alternative sources of energy other than oil, for example, wind, solar and geothermal energy, and tidal ,Which it the right direction, and start racing to dispense with fossil fuels in the coming years. The concept of energy use in the world is shown in Figure 1.2

1.3 Effects of Fossil Fuel Combustion on Environment

Fossil fuels are the main primary source for electrical power generation and heat generation and include petroleum, natural gas, and coal. All these fuels contain hydrogen, oxygen, carbon, sulfur, and nitrogen compounds.

During the fossil fuels burning the exhaust gas which has a harmful impact on the environment and living creatures. Some of these gases are greenhouse gases, including but not limited to such H_2O, CO_2, and NOx.

Climate change associated with rising atmospheric CO_2 has already carbon balance through rising temperature, increasing growing season, and increased atmospheric water content.

Nitrogen dioxide is an irritant gas, when the fuel combustion the nitrogen combines with the atoms of oxygen to produce nitric oxide (NO) which is harmful to environment.

1.4 Aims and Objectives

Due to the increased energy demand and environmental concerns, it is necessary to find alternative ways for supplying the energy needs. One alternative way is a multigeneration system which is used to supply multiple forms of energy. Multigeneration systems are having higher efficiencies than conventional system. The main point of this study is to analyze a multi generation systems which delivers electricity, cooling, heating and hydrogen that could be used as fuel in advanced systems. It is aimed to do parametric study; vary some parameters and observe the others. The proposed system in this study includes sub systems of double effect

absorption cooling system and two-stage Rankine Cycle based power producing system for covering demands of cooling, heating and electricity.

The study aims to analyze all the system in both energetic and exergetic point of view. It is aimed to do energetic and exergetic analysis for every device existing in the system.

Chapter 2

LITERATURE REVIEW

2.1 Introduction

In spite of numerous investigation and studies conducted to explore the performance and viability of cogeneration (simultaneous electricity and heat production) and tri-generation (simultaneous electricity, heat and cooling production) energy systems, very few comprehensive researches has been done on the performance of multi-generation energy systems. This literature review is about the recent research on cogeneration, tri-generation and multigeneration energy systems.

2.2 Cogeneration System

Heat and electricity production, combined heat and power or cogeneration is the concurrent. Large amount of heat is produced but not used in ordinary power plants. The efficiency of energy production can be increased from current levels that range from 35% to 55%, to over 80%, by designing systems that can use the heat (DOE, 2003).

In cogeneration, energy source is usually fossil fuel or uranium and thermal energy in cogeneration is produced from the steam or hot water and used especially in industry [4].

Burning fuel to produce high pressure steam inter turbine generate electricity. The low pressure steam can be used for useful.

Thermal energy, various fuels can be used in steam turbines, such as coal, wood, solid waste and natural gas.

There is the beginning of the development of fuel cells and small markets and combined heat and power (CHP) applications. [4]

2.3 Multi Generation

Multi generation is also called poly generation. Multi-generation is achieved by merging operations at one time with a rush out into account use a single or more than one source of energy. Multi-generations is utilizes the power wasted by generating power plants, especially in cooling and heating. The purpose of the use of multi-generation full utilization of fuel and reduce wasted energy as much as possible is the way to improve the process of power generation. Fuel consumption is less to produce a certain amount of electric or thermal energy as opposed to produce this amount in the traditional manner discrete (e.g. turbines and boilers Group) .In addition, multi generation systems integrated with drying processes or can be integrated with an electrolyzer can produce hydrogen [5].

Multi-generation system, the latest quantum leap in power plants where is it is possible to add systems for other non-electricity output. This type of system should be considered residential applications, generating stations of the ability to require the beneficial outcomes and a clear sense that if there is an urgent need for cooling somewhere means multi generation system must give priority to this application [6]. Multi generation system is a viable problem of pollution and global warming solutions in modern times. Is the multi generation is a relatively new way, using a single source and in turn get boiled several outputs [5]. Generating saturated steam is necessary to enter the turbine using a heat recovery steam generator; to produce

electricity on the other hand works the low vapor pressure as an absorption cooling heat input into the generator.

2.4 Review of the Studies on Multi Generation Systems

Thermodynamic analysis of multi generation systems was done by many researches in the literature. Maidment and Tozer (2002) [7] analyzed five different systems of tri-generation in supermarkets integrated with absorption chillers. The results from the energy analysis illustrated that huge amount of energy savings can be achieved with decrease in carbon dioxide emissions compared to conventional coal and gas energy systems for electricity generation.

Tracy et al. (2007).[8] thermodynamically analyzed the effect of the waste heat of a tri-generation system respectively between heating and cooling process based on first and second laws of thermodynamics. Huang fu et al. (2007a). [9] studied a small size of a tri-generation system, integrated with an adsorption chiller cooling system. They have done economic and energy analyses of the system. In the exergetic analysis, they presented an enhancement of the engine electrical efficiency reasons an upgrading of the tri-generation system operation.

Numerous projects were analyzed about gas turbines as a prime mover for cogeneration and tri-generation energy systems. A primary concept for various gas turbine was established by Calva et al.(2005).[10] Their system debated the design of tri-generation energy systems. Ziher and Poredos (2006) [11] did economic analysis on a tri-generation system for a hospital building. Steam absorption joined with compression cooling system integrated with cold storage capability was planned for cooling purposes. An exergy analysis was done on a tri-generation energy system based on a gas turbine by Khaliq and Kumar (2008). [12] They examined the effect

of compressor pressure ratio variation and process heat pressure on first and second law efficiencies and electrical to thermal energy ratio. Khaliq (2009) [13] studied the same system to check the effect of turbine inlet temperature variation, pressure drop percentage of combustion chamber and heat recovery steam generator (HRSG) and evaporation temperature. The results showed that combustion and steam generation gives with more than 80% of the exergy destruction.

Jaaskelainen and Wallace (2009) [14] conducted energy and economic analyses for a tri-generation system run by a micro-turbine with the capacity of 240 kW. The economic analysis of this system presented that it is not feasible to use the designed micro-turbine because of low electricity rates due to the natural gas price. Medrano et al.(2006). [15] Conducted a complete exergy analysis of three different tri-generation integrated energy systems. The proposed systems are joined to a single effect, a double effect and combined single and double effect absorption chillers. They concluded that exergy efficiency difference of the proposed plants is less than 1%. Liang and Wang (2007).[16] examined a study on micro-turbine based tri-generation system. They assessed the exergetic efficiency in an integration of double effect absorption chiller for cooling purpose. They presented exergetic comparative analysis done by the exergetic efficiency of the designed system with a system that consumes electrical chiller as an alternative. It was shown that tri-generation energy system with absorption chiller is working in higher exergetic efficiency range Buck and Fredmann (2007) [17] analyzed a tri-generation energy system linked to micro-turbine and assisted by small solar tower. Their study measured the economics aspects of using single and double effect absorption chiller which shows a strong improvement of the system operation and lower operating charge, with respect to single effect absorption chiller. A huge amount of saving in energy and decrease in

carbon dioxide emissions are stated by Medrano et al. (2008) [18] when solar thermal collectors were utilized to feed the production of heating and cooling produced by tri-generation integrated energy system operated by an internal combustion engine. There are several recent studies on solar based tri- and multi-generation systems. Cho et al. (2014) [19] showed a complete review on conventional and unconventional combined heat and power (CHP) and combined cooling, heat and power (CCHP) energy systems. Most current works with their key factors have been argued in detail. Al-Sulaiman et al. (2011) [20] displayed a new solar based tri-generation system using exergetic analysis. Rosiek and Batlles (2013) [21] examined solar-based building cooling, heating and power generation applications building cooling heating and power (BCHP). A new combined cooling heating and power (CCHP) energy system was designed by Wang et al. (2012) [22]and parametric study was done to check the performance of the system working with a trans critical CO2 cycle using solar energy as the heat input. Meng et al. (2010) [23]showed a solar based combined cooling heating and power (CCHP) plant with extra input of industrial waste heat, to produce power and cooling. Ozcan and Dincer (2013) [24]presented a parametric study for a tri-generation system using the waste heat from the solid oxide fuel cell (SOFC) system and solar energy as the assisting energy source for an integrated RC plant.

Limited researches were done by considering plants with multi-prime movers. A novel integrated tri-generation plant with micro gas turbine, solid oxide fuel cell (SOFC) and single effect absorption chiller was designed by Velumani et al. (2010). [25]The results illustrate that the energetic efficiency of the proposed cycle is about 70%. The feasibility of the mentioned energy system was checked through cost

analysis. Chung Tse et al. (2011) [26] studied the performance of a tri-generation system based on solid oxide fuel cell (SOFC) and gas turbine for marine demands.

Numerous researches in the journalism analyzed the biomass gasification. Schuster et al. (2001) [27] presented a comprehensive parametric study on a double stage steam for combined heat and power (CHP). They investigated the effect of the gasification temperature, fluidization agent and water on the performance of the system. Cohce et al. (2011) [28] did an efficiency analysis for biomass gasification system for hydrogen production. They defined a simple prototype for energetic and exergetic analysis considering chemical equilibrium.

RC is a suitable option for integrated systems and multi-generation plants. Significant research has been done to evaluate the performance assessment of the Rankine Cycle that is integrated to geothermal and solar energy sources. Scientists analyzed the possibility of a suitable working fluid, optimal reinjection condition of the geothermal fluid, the ability of cogeneration and the economic analysis of such a system.

From the literature, one can see that there are several researches on the analysis of cogeneration and tri-generation energy systems. However, not enough research has been conducted on multigeneration energy systems, especially, renewable based multigeneration systems.

Chapter 3

SYSTEM DESIGN

3.1 System Topology

The multi-generation system considered in this work exploits a geothermal energy source to run a double effect absorption cooling system and, Rankine cycle. The purpose of this system is to generate electric power, cooling, and heating to be used in residential sector. It is also aimed to use portion of the produced electricity for hydrogen generation. The system topology can be seen in Figure 3.1. The system description is given in below sections.

3.1.1 Rankine Cycle

In this multi generation system Rankine Cycle based turbine is proposed for electricity generation .The working fluid in RC is water. The end point of a phase equipoise curve must have a high critical point (critical state), to ensure a high efficient RC. Liquid –vapor critical temperature and pressure are 373.946℃ and 22.06 MP for water, and T-S diagram of water is showed in Figure 3.2.

In state 33 the water enters to the pump as saturated liquid then compressed isentropically. In state 34 the compressed liquid enters to heat exchanger, exchanges heat with the fluid which is coming from the geothermal source, and leaves at state 29 as superheated vapor.

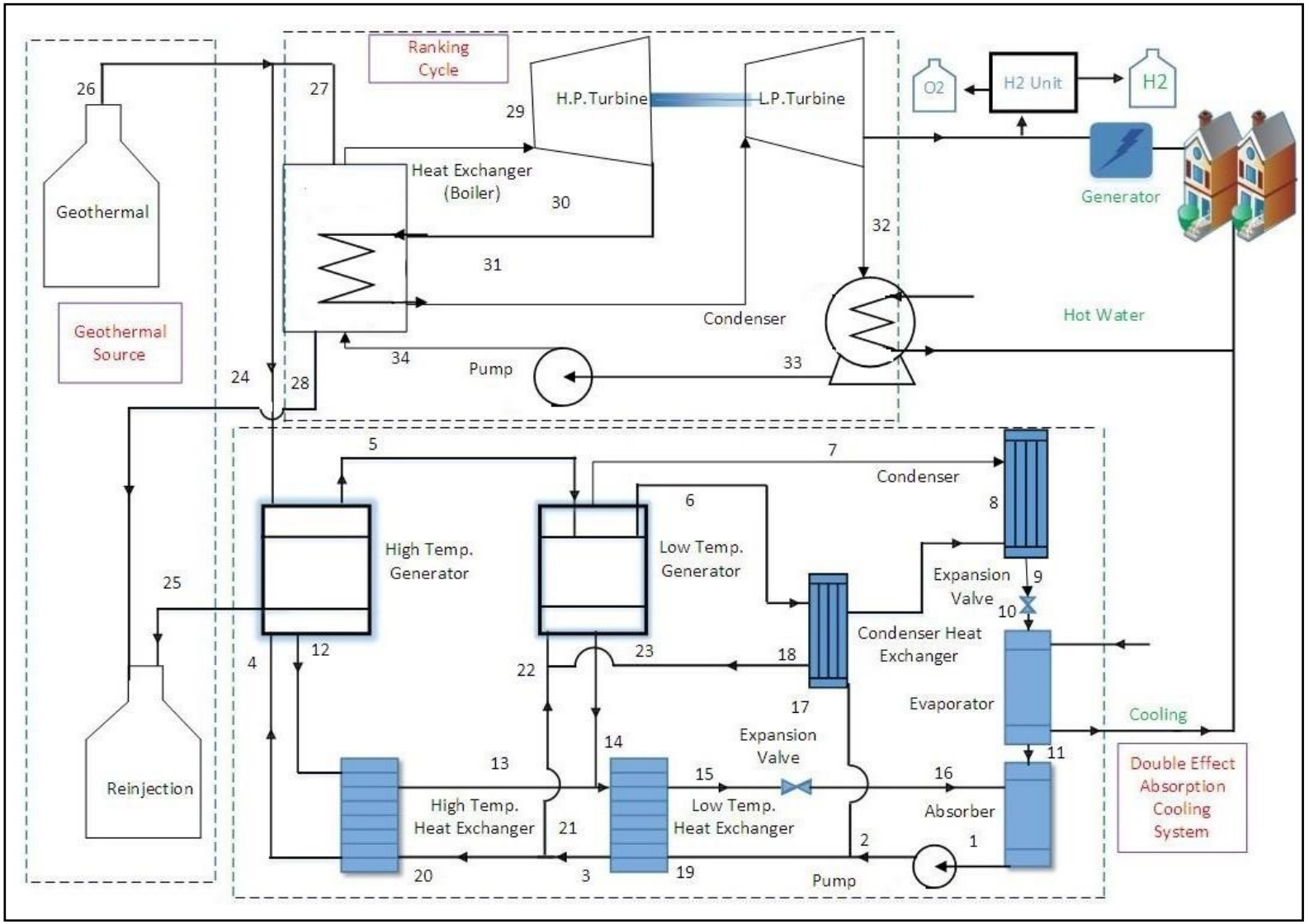

Figure 3.1: Diagram of integrated for multi-generation system geothermal energy based

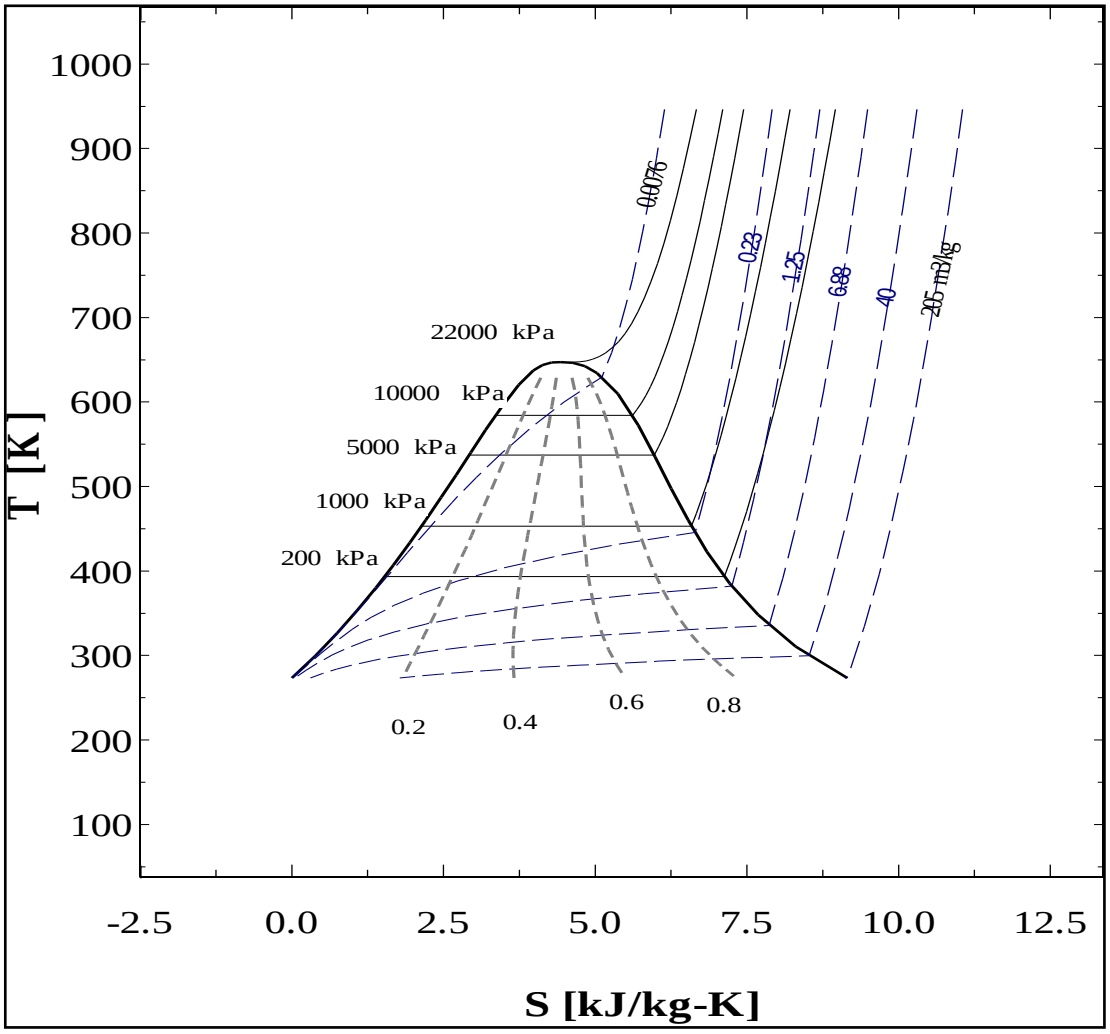

Figure 3.2: T-S diagram of water [29]

In state 29 steams enters to high pressure turbine and expands isentropically and returns back to the heat exchanger to be reheated at constant pressure. After reheat process it enters into low pressure turbine, and expands isentropically. At the end of this process mechanical work occurs in terms of rotating shaft.

In state 32 steams enter to the condenser with lower pressure and temperature. Steam has high quality and usually is in the state of saturated liquid –vapor mixture and rejects heat then the steam leaves as saturated liquid from the condenser.

3.1.2 Double Effect Absorption Cooling System

In the double effect absorption cooling system (DEACS), in this system the Lithium bromide water as working fluid. In the middle of the 20^{th} century the LiBr-water became fluid trading as water chiller for huge building air-conditioning, and become widely used because of non-toxic and environmentally friendly .However, it should be considered that LiBr-H_2O but you cannot be used for applications that require sub zero temperatures.

The system of double effect absorption cooling (DEACS) consists of a pump, an evaporator, an absorber, a low temperature heat exchanger, a high temperature heat exchanger, a high temperature generator, a low temperature generator, a condenser, and a condenser heat exchanger. In DEACS, the high temperature generator receives the heat from geothermal source increasing the temperature and vaporizing the weak solution at state 4.The strong solution at state 12 and at state 5 exits as a water vapor. In state 20 transferred heat to the weak quality solution passed across strong quality solution from high temperature heat exchanger In low temperature heat exchanger strong solution enter to release heat to weak solution at state 14 then leaves at state 15 which strong solution enter to expansion valve where pressure reducing and pass to absorber at state 16. The condenser heat exchanger decrease the temperature of water vapor entering at state 6 then increase the temperature of weak solution at state 17.In the condenser heat rejected to the environment then leave at state 9, in the expansion valve the vapor water entering during decreasing pressure and temperature then enter to the evaporator at state 10. In state 11 leave as water vapor and state 16 as lithium bromide water mixture entering the absorber where rejected heat to the environment then enter to the pump at state 1 as lithium bromide-water solution.

3.2 Energy and Exergy Analysis

In multi-generation system energy and exergy calculations were presented by using the entrance and exit thermodynamic properties for each equipment. Exergy destructions are calculated also which shows the irreversibilities system. The energy and exergy balances for the multi-generation system are presented as below:

3.2.1 RC Pump

The pump of RC is illustrated in Figure 3.3.

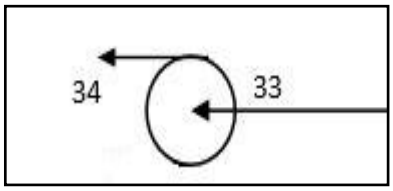

Figure 3.3: Schematic diagram pump of RC

The pump work required ($\dot{W}_{RC\ pump}$) is written by applying in the equation as below:

$$\dot{W}_{RC\ pump} = (\dot{m}_{33} * v_{33}(p_{34} - p_{33}))/0.8 \quad \text{(kW)} \quad (1)$$

where $\dot{m}$ is the mass flow rate, v is the specific volume and p is the pressure.

The number 0.8 is for accounting the irriversibilities in the pump and it is the isentropic efficiency of the pump.

The exergy destruction of the pump ($\dot{E}x_{dest\ RC\ pump}$) can be evaluated as below:

$$\dot{E}x_{dest\ RC\ pump} = \dot{m}_{33} ex_{33} + \dot{W}_{RC\ pump} - \dot{m}_{34} ex_{34} \quad \text{(kW)} \quad (2)$$

where ex is the exergy.

3.2.2 RC High Pressure Turbine

In state 29 high temperature working fluid (super heated) enters to turbine and leaves the turbine at state 30 after the expansion, the high pressure turbine of RC is illustrated in Figure 3.4.

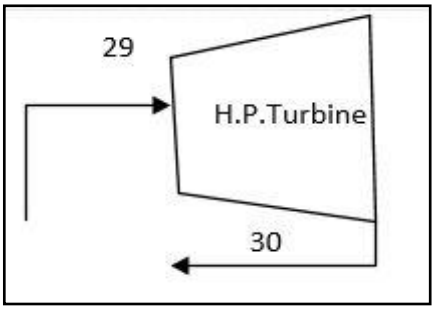

Figure 3.4: Schematic diagram of RC high pressure turbine

Work output of the high pressure turbine ($\dot{W}_{RC\ hpt}$) is evaluated as below:

$$\dot{W}_{RC\ hpt} = (\dot{m}_{29}h_{29} - \dot{m}_{30}h_{30}) * 0.87 \quad \text{(kW)} \quad (3)$$

where h is the enthalpy and number 0.87 is for accounting the irriversibilities in the high pressure turbine and it is the efficiency isentropic

In high pressure turbine the exergy destruction ($\dot{E}x_{dest\ RC\ hpt}$) can be shown by applying in exergy equation as below:

$$\dot{E}x_{dest\ RC\ hpt} = \dot{m}_{29}ex_{29} - \dot{m}_{30}ex_{30} + \dot{W}_{RC\ hpt} \quad \text{(kW)} \quad (4)$$

3.2.3 RC Low Pressure Turbine

The low pressure turbine of RC is illustrated in Figure 3.5.

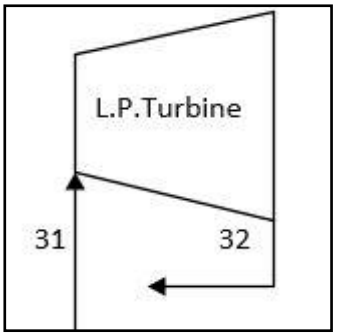

Figure 3.5: Schematic diagram of RC low pressure turbine

The work output of low pressure turbine ($\dot{W}_{RC\ lpt}$) can be calculated as follows:

$$\dot{W}_{RC\ lpt} = (\dot{m}_{31}h_{31} - \dot{m}_{32}h_{32}) * 0.989 \quad \text{(kW)} \quad (5)$$

The number 0.989 is for accounting the irriversibilities in the low pressure turbine and it is the isentropic efficiency.

The exergy destruction balance equation of low pressure turbine ($\dot{E}x_{dest\ RC\ lpt}$) can be written as:

$$\dot{E}x_{dest\ RC\ lpt} = \dot{m}_{31}ex_{31} - \dot{m}_{32}ex_{32} + \dot{W}_{RC\ lpt} \quad \text{(kW)} \quad (6)$$

3.2.4 RC Condenser

The condenser of RC is illustrated in Figure 3.6.

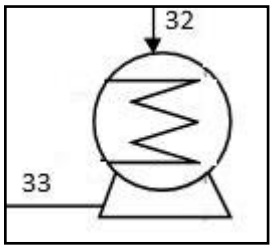

Figure 3.6: Schematic diagram of RC condenser

The energy Heat of RC condenser ($\dot{Q}_{RC\ cond}$), exergy heat of RC Condenser ($\dot{E}xq_{RC\ cond}$) and exergy destruction of RC condenser ($\dot{E}x_{dest\ RC\ cond}$) can be calculated as below:

$$\dot{Q}_{RC\ cond} = \dot{m}_{32}h_{32} - \dot{m}_{33}h_{33} \quad \text{(kW)} \quad (7)$$

$$\dot{E}xq_{RC\ cond} = (1 - T_0)/(T_{32}/2 + T_{33}/2) * \dot{Q}_{RC\ cond} \quad \text{(kW)} \quad (8)$$

$$\dot{E}x_{dest\ RC\ cond} = \dot{m}_{32}ex_{32} - \dot{m}_{33}ex_{33} - \dot{E}xq_{RC\ cond} \quad \text{(kW)} \quad (9)$$

3.2.5 RC Heat Exchanger

In this component, heat is transferred from geothermal high temperature to high pressure turbine Rankine cycle then reheated to inter low pressure turbine and working fluid is water. The heat exchanger of RC is illustrated in Figure 3.7.

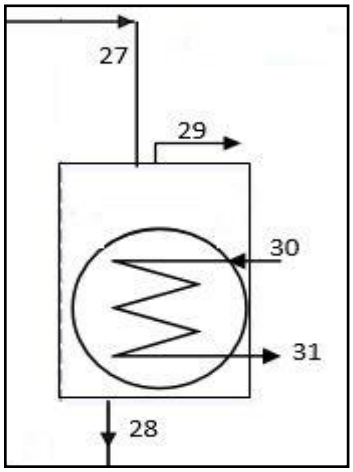

Figure 3.7: Schematic diagram of RC heat exchanger

Energy ($\dot{Q}_{RC\ he}$), exergy ($\dot{Exq}_{RC\ he}$) and exergy destruction Heat transfer rate of the heat exchanger ($\dot{E}x_{dest\ RC\ he}$) can be shown as below:

$$\dot{Q}_{RC\ he} = -\dot{m}_{31}h_{31} + \dot{m}_{27}h_{27} - \dot{m}_{28}h_{28} - \dot{m}_{29}h_{29} + \dot{m}_{34}h_{34} + \dot{m}_{30}h_{30}$$

(kW) (10)

$$\dot{E}xq_{RC\ he} = (1 - T_0)/(T_{27}/6 + T_{28}/6 + T_{30}/6 + T_{29}/6 + T_{31}/6 + T_{34}/6) * \dot{Q}_{RC\ he}$$

(kW) (11)

$$\dot{E}x_{dest\ RC\ he} = -\dot{m}_{31}ex_{31} + \dot{m}_{27}ex_{27} - \dot{m}_{28}ex_{28} + \dot{m}_{29}ex_{29} - \dot{m}_{34}ex_{34} +$$

$$\dot{m}_{30}30_{30} - \dot{E}xq_{RC\ he} \quad \text{(kW)} \quad (12)$$

3.2.6 RC Efficiency

The total work and net work for the RC ($\dot{W}_{RC\ net}$) can be calculated by using fallowing expressions:

$$\dot{W}_{RC\ total} = \dot{W}_{RC\ lpt} + \dot{W}_{RC\ hpt} \quad \text{(kW)} \quad (13)$$

$$\dot{W}_{RC\ net} = \dot{W}_{RC\ total} - \dot{W}_{RC\ pump} \quad \text{(kW)} \quad (14)$$

Thermal (η_{th}) and exergy (Ψ_{th}) efficiencies of Rankine Cycle are given in equations below:

$$\eta_{th} = \frac{\dot{W}_{RC\ net}}{\dot{Q}_{RC\ he}} \quad \text{(kW)} \quad (15)$$

$$\Psi_{th} = \frac{\dot{W}_{RC\ net}}{\dot{E}xq_{RC\ he}} \quad \text{(kW)} \quad (16)$$

3.2.7 Double Effect Absorption Cooling System

3.2.7.1 Pump

The pump of DEACS is illustrated in Figure 3.8

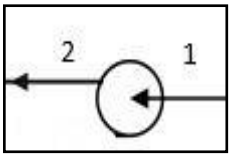

Figure 3.8: Schematic diagram of pump

The pump work required ($\dot{W}_{DEACS\ pump}$) is written by applying in the equation as below:

$$\dot{W}_{DEACS\ pump} = \dot{m}_1(h_2 - h_1)/0.85 \quad \text{(kW)} \quad (17)$$

The number 0.85 is for accounting the irriversibilities and it is the isentropic efficiency.

The exergy destruction of the pump ($\dot{E}x_{dest\ DEACS\ pump}$) can be evaluated as below:

$$\dot{E}x_{dest\ DEACS\ pump} = \dot{m}_1 ex_1 + \dot{W}_{DEACS\ pump} - \dot{m}_2 ex_2 \quad \text{(kW)} \quad (18)$$

3.2.7.2 Low Temperature Heat Exchanger

The low Temperature Heat Exchanger of DEACS cycle is illustrated in Figure 3.9

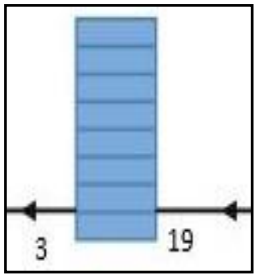

Figure 3.9: Schematic diagram of low temperature heat exchanger

Energy heat balance of the low temperature heat exchanger ($\dot{Q}_{DEACS\ lhx}$) is given as below:

$$\dot{Q}_{DEACS\ lhx} = \dot{m}_3 h_3 - \dot{m}_{19} h_{19} \quad \text{(kW)} \quad (19)$$

Exergy heat of low temperature heat exchanger ($\dot{E}xq_{DEACS\ lhx}$) can be written as below:

$$\dot{E}xq_{DEACS\ lhx} = (1 - T_0)/(T_{19}/2 + T_3/2) * \dot{Q}_{DEACS\ lhx} \quad \text{(kW)} \quad (20)$$

The exergy destruction of the low temperature heat exchanger ($\dot{E}x_{dest\ DEACS\ lhx}$) can be written as below:

$$\dot{E}x_{dest\ DEACS\ lhx} = \dot{m}_{19} ex_{19} - \dot{m}_3 ex_3 - \dot{E}xq_{DEACS\ lhx} \quad \text{(kW)} \quad (21)$$

3.2.7.3 High Temperature Heat Exchanger

The high Temperature Heat Exchanger of DEACS is illustrated in Figure 3.10

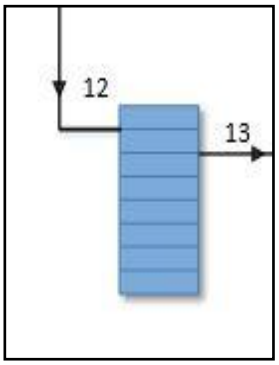

Figure 3.10: Schematic diagram of high temperature heat exchanger

Heat balance of high temperature heat exchanger ($\dot{Q}_{DEACS\ hhx}$) can be applied as below:

$$\dot{Q}_{DEACS\ hhx} = \dot{m}_{12} h_{12} - \dot{m}_{13} h_{13} \quad \text{(kW)} \quad (22)$$

Exergy ($\dot{E}xq_{DEACS\ hhx}$) and Exergy destruction ($\dot{E}x_{dest\ DEACS\ hhx}$) of high temperature heat exchanger can be written as below:

$$\dot{E}xq_{DEACS\ hhx} = (1 - T_0)/(T_{12}/2 + T_{13}/2) * \dot{Q}_{DEACS\ hhx} \quad \text{(kW)} \quad (23)$$

$$\dot{E}x_{dest\ DEACS\ hhx} = \dot{m}_{12}ex_{12} - \dot{m}_{13}ex_{13} - \dot{E}xq_{DEACS\ hhx} \quad \text{(kW)} \quad (24)$$

3.2.7.4 High Temperature Generator

The high Temperature Generator of DEACS cycle is illustrated in Figure 3.11

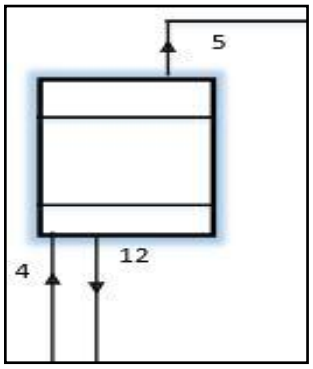

Figure 3.11: Schematic diagram of high temperature generator

Energy heat balance of high temperature generator ($\dot{Q}_{DEACS\ htg}$) can be written as below:

$$\dot{Q}_{DEACS\ htg} = \dot{m}_5 h_5 + \dot{m}_{12} h_{12} - \dot{m}_4 h_4 \quad \text{(kW)} \quad (25)$$

Exergy ($\dot{E}xq_{DEACS\ htg}$) and exergy destruction ($\dot{E}x_{dest\ DEACShtg}$) of high temperature generator are expressed as below:

$$\dot{E}xq_{DEACS\ htg} = (1 - T_0)/(T_{12}/3 + T_5/3 + T_4/3) * \dot{Q}_{DEACS\ htg} \quad \text{(kW)} \quad (26)$$

$$\dot{E}x_{dest\ DEACShtg} = \dot{m}_4 ex_4 - \dot{m}_5 ex_5 - \dot{m}_{12} ex_{12} - \dot{E}xq_{DEACS\ htg} \quad \text{(kW)} \quad (27)$$

3.2.7.5 Low Temperature Generator

The low Temperature Generator of DEACS cycle is illustrated in Figure 3.12

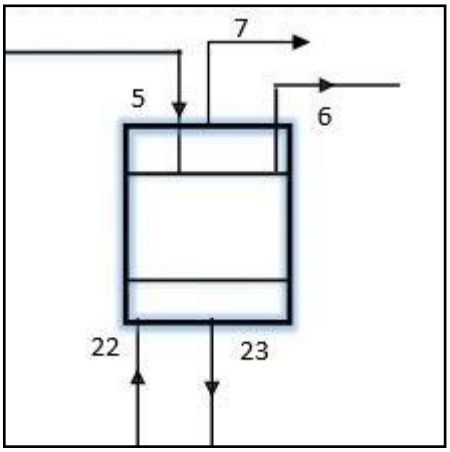

Figure 3.12: Schematic diagram of low temperature generator

Heat balance of low Temperature Generator can be written as below:

$$\dot{Q}_{DEACS\ ltg} = \dot{m}_{23}h_{23} + \dot{m}_{6}h_{6} + \dot{m}_{7}h_{7} - \dot{m}_{22}h_{22} - \dot{m}_{5}h_{5} \quad \text{(kW)} \quad (28)$$

Exergy ($\dot{E}xq_{DEACS\ ltg}$) and exergy destruction ($\dot{E}x_{dest\ DEACSltg}$) are given as below:

$$\dot{E}xq_{DEACS\ ltg} = (1 - T_0)/(T_{23}/5 + T_6/5 + T_7/5 + T_{22}/5 + T_5/5) * \dot{Q}_{DEACS\ ltg}$$

(kW) (29)

$$\dot{E}x_{dest\ DEACSltg} = -\dot{m}_{6}ex_{6} - \dot{m}_{23}ex_{23} - \dot{m}_{7}ex_{7} + \dot{m}_{22}ex_{22} - \dot{m}_{5}ex_{5} +$$

$\dot{E}xq_{DEACS\ ltg}$ (kW) (30)

3.2.7.6 Condenser Heat Exchanger

The condenser Heat Exchanger of DEACS cycle is illustrated in Figure 3.13

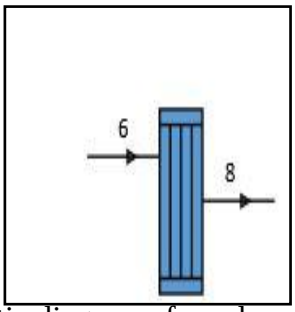

Figure 3.13: Schematic diagram of condenser heat exchanger

Energy balance of condenser Heat Exchanger is given as below:

$$\dot{Q}_{DEACS\ che} = -\dot{m}_6 h_6 + \dot{m}_8 h_8 \quad \text{(kW)} \quad (31)$$

The exergy ($\dot{E}xq_{DEACS\ che}$) and exergy destruction ($\dot{E}x_{dest\ DEACSche}$) are written as below:

$$\dot{E}xq_{DEACS\ che} = (1 - T_0)/(T_8/2 + T_6/2) * \dot{Q}_{DEACS\ che} \quad \text{(kW)} \quad (32)$$

$$\dot{E}x_{dest\ DEACSche} = \dot{m}_6 ex_6 - \dot{m}_8 ex_8 - \dot{E}xq_{DEACS\ che} \quad \text{(kW)} \quad (33)$$

3.2.7.7 Condenser

The condenser of DEACS cycle is illustrated in Figure 3.14

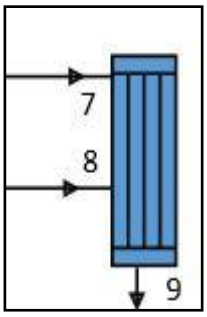

Figure 3.14: Schematic diagram of condenser

An energy balance for the condenser ($\dot{Q}_{DEACS\ cond}$) follows:

$$\dot{Q}_{DEACS\ cond} = \dot{m}_7 h_7 + \dot{m}_8 h_8 - \dot{m}_9 h_9 \quad \text{(kW)} \quad (34)$$

Exergy ($\dot{E}xq_{DEACS\ cond}$) and exergy destruction of condenser ($\dot{E}x_{dest\ DEACS\ COND}$) can be written as below:

$$\dot{E}xq_{DEACS\ cond} = (1 - T_0)/(T_7/3 + T_8/3 + T_9/3) * \dot{Q}_{DEACS\ cond}$$

(kW) (35)

$$\dot{E}x_{dest\ DEACS\ COND} = \dot{m}_7 ex_7 + \dot{m}_8 ex_8 - \dot{m}_9 ex_9 - \dot{E}xq_{DEACS\ cond} \quad \text{(kW)} \quad (36)$$

3.2.7.8 Evaporator

The evaporator of DEACS cycle is illustrated in Figure 3.15

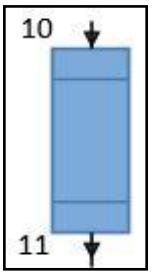

Figure 3.15: Schematic diagram of evaporator

Energy balance for the evaporator ($\dot{Q}_{DEACSevap}$) can is expressed as below:

$$\dot{Q}_{DEACSevap} = \dot{m}_{11}h_{11} - \dot{m}_{10}h_{10} \quad \text{(kW)} \quad (37)$$

Exergy ($\dot{E}xq_{DEACSevap}$) and exergy destruction ($\dot{E}x_{dest\ DEACS\ evap}$) for the evaporator are written as below:

$$\dot{E}xq_{DEACSevap} = (1 - T_0)/(T_{10}/2 + T_{11}/2) * \dot{Q}_{DEACSevap} \quad \text{(kW)} \quad (38)$$

$$\dot{E}x_{dest\ DEACS\ evap} = \dot{m}_{10}ex_{10} - \dot{m}_{11}ex_{11} - \dot{E}xq_{DEACSevap} \quad \text{(kW)} \quad (39)$$

3.2.7.9 Absorber

The absorber of DEACS cycle is illustrated in Figure 3.16

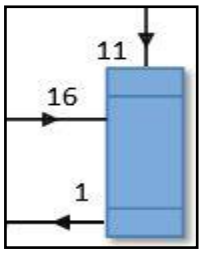

Figure 3.16: Schematic diagram of absorber

Heat rejected from the absorber ($\dot{Q}_{DEACS\ abs}$) can be shown by using energy equation as below:

$$\dot{Q}_{DEACS\ abs} = \dot{m}_{11}h_{11} + \dot{m}_{16}h_{16} + \dot{m}_1h_1 \quad \text{(kW)} \quad (40)$$

Exergy ($\dot{E}xq_{DEACS\ abs}$) and exergy destruction ($\dot{E}x_{dest\ DEACS\ abs}$) are determined as follows:

$$\dot{E}xq_{DEACS\ abs} = (1 - T_0)/(T_{11}/3 + T_{16}/3 + T_1/3) * \dot{Q}_{DEACS\ abs} \quad \text{(kW)} \quad (41)$$

$$\dot{E}x_{dest\ DEACS\ abs} = \dot{m}_{11} ex_{11} + \dot{m}_{16} ex_{16} - \dot{m}_1 ex_1 - \dot{E}xq_{DEACS\ abs} \quad \text{(kW)} \quad (42)$$

3.2.7.10 Total COP

The energetic COP for the DEACS can be given as below:

$$COP_{EN} = \dot{Q}_{DEACS\ evap} / (\dot{Q}_{DEACS\ htg} + \dot{W}_{DEACS\ pump}) \quad (43)$$

The exergetic COP for the DEACS can be written as below:

$$COP_{EX} = -\dot{E}xq_{DEACS\ evap} / (\dot{E}xq_{DEACShtg} + \dot{W}_{DEACS\ pump}) \quad (44)$$

3.2.7.11 Electrolyzer

The electrolyzer is the one readily available in the market which uses electricity to disconnect water particle. The value of hydrogen produced by the electrolyzer can be calculated as below:

$$\dot{M}H_2 = \frac{\eta_{elec} \times 0.4\ \dot{W}_{RC\ net}}{HHV} \quad (45)$$

Where is η_{elec} 55% and, high heating value for hydrogen (HHV) is 141800kJ/kg.

3.2.7.12Utilization Factor

The utilization factor can be calculated as below:

$$\in_U = (\dot{W}_{RC\ net} + \dot{Q}_{DEACS\ evap} + \dot{E}x_{dest\ DEACS\ cond} + (\dot{M}H_2 * h_{H2}))/\dot{Q}in \quad (46)$$

Where is $\dot{M}H_2$ amount of hydrogen production (kg/s), h_{H2} the enthalpy of hydrogen (kJ/kg).

Chapter 4

DATA ANALYSIS

In the energy and exergy analyses of the proposed renewable energy (geothermal water) based integrated multigeneration system, values of mass flow rate (kg/s), temperature (°C), pressure (kPa), specific enthalpy (kJ/kg), has been evaluated and results are presented in the table 1. The reference conditions are taken to be the conditions of the ambient where P_0 = 101.325 kPa, and T_0 = 25 °C. Thermodynamic properties are calculated by using Engineering Equation Solver (EES) software which is powerful software for thermodynamic analysis.

The overall RC energetic and exergetic efficiencies for the Rankine Cycle are evaluated as 12.16% and 16.21%, respectively. The double effect absorption cooling system COP is 1.437; this is much higher than the exergetic COP which is 0.3371 due to the exergy destruction in exergetic analysis.

A parametric study is dined to present the effect of inlet pressure and temperature on the total efficiency of the system. Table 2 presents some vital system parameters such as pumps work RC turbines produced work, energetic and exergetic COPs in DEACS (Double Effect Absorption Cooling System) and etc. In order to enhance the system performance quality, some affect in parameters such as inlet pressure and turbine temperature are varied, these parameters as the important design factors are discussed in more detail as below.

Table 4.1: Thermodynamic Properties of the System at Each State

State	T($K°$)	P(kPa)	ṁ(kg/s)	h(kJ/kg)	S(kJ/kg.K)	Ex(kJ/kg)	X(-)	V(m^3/kg)
0	298	101	-	298.4	5.696	-	-	-
1	303.5	0.86	0.5	68.19	0.1945	1409	0.5291	-
2	303.8	8.4	0.5	128.4	0.4455	1395	0.0001	-
3	320	8.4	0.4	128.2	0.5454	1365	0.2573	-
4	365	8.4	0.32	225.6	0.5045	1474	0.6169	-
5	375	8.4	0.1069	2691	8.537	1545	-	-
6	317	8.4	0.1069	2580	8.218	1530	-	-
7	338	8.4	0.0601	2620	8.34	1534	-	-
8	300	8.4	0.1069	112.5	0.3928	1394	-	-
9	300	8.4	0.167	112.5	0.3928	1394	-	-
10	279	0.95	0.167	24.59	0.08907	1397	-	-
11	280	0.86	0.167	2513	9.043	1217	-	-
12	353	8.4	0.2132	179.9	0.4815	1435	0.5623	-
13	347	8.4	0.2132	160.8	0.4736	1419	0.5329	-
14	319	8.4	0.3331	132	0.5543	1366	0.2231	-
15	280	8.4	0.3331	28.76	0.1041	1397	0.0001	-
16	350	0.86	0.3331	292.9	0.3124	1599	0.7548	-
17	323	8.4	0.1	122.6	0.52	1367	0.3301	-
18	313	8.4	0.1	166.8	0.5702	1396	0.0001	-
19	355	8.4	0.4	186.9	0.4849	1441	0.5717	-
20	333	8.4	0.32	128.5	0.4768	1385	0.4469	-
21	332	8.4	0.08	127	0.4789	1383	0.4389	-
22	365	8.4	0.18	225.6	0.5045	1474	0.6169	-
23	302	8.4	0.1199	120.8	0.4206	1394	0.0001	-
24	478	900	3	2844	6.775	2224	-	-
25	348	900	3	314	1.013	1411	-	-
26	478	900	4	2844	6.775	2224	-	-
27	450	900	1	2777	6.63	2200	-	-
28	383	900	1	461.3	1.416	1438	-	-
29	449	900	9	2775	6.625	2200	-	-
30	373	20	9	2685	8.124	1663	-	-
31	363	20	9	2666	8.072	1660	-	-
32	325	10	9	2595	8.184	1555	-	-
33	274.3	10	9	191.8	0.6493	1397	-	0.0010001
34	320	900	9	192.7	0.6624	1394	-	-

Table 4.2: Output Values of Components.

Component	Values	Component	Values
COP_{En}	1.437	Exq_{HTG}	46.21 [kJ/s]
COP_{Ex}	0.3371	Exq_{LHX}	-2.747 [kJ/s]
EfficiencyEX	16.21%	Exq_{LTG}	14.59 [kJ/s]
EfficiencyTH	12.67%	$ExqRC_{CON}$	120.3 [kJ/s]
$Exdest_{ABS}$	10.82 [kJ/s]	$ExqRC_{HEX}$	-4881 [kJ/s]
$Exdest_{CHX}$	23.52 [kJ/s]	Q_{ABS}	483.2 [kJ/s]
$Exdest_{CON}$	1.321 [kJ/s]	Q_{CHX}	-263.8 [kJ/s]
$Exdest_{EVAP}$	152.1 [kJ/s]	Q_{CON}	150.7 [kJ/s]
$Exdest_{HHX}$	4.19 [kJ/s]	Q_{EVA}	415.6 [kJ/s]
$Exdest_{HTG}$	46.71 [kJ/s]	Q_{HHX}	4.084 [kJ/s]
$Exdest_{LHX}$	27.94 [kJ/s]	Q_{HTG}	253.8 [kJ/s]
$Exdest_{LTG}$	22.16 [kJ/s]	Q_{LHX}	-23.47 [kJ/s]
$Exdest_{PUMP}$	42.7 [kJ/s]	Q_{LTG}	119.6 [kJ/s]
$ExdestRC_{CON}$	1302 [kJ/s]	QRC_{CON}	21631 [kJ/s]
$ExdestRC_{HEX}$	12924 [kJ/s]	QRC_{HEX}	-20196 [kJ/s]
$ExdestRC_{HPT}$	4021 [kJ/s]	W_{NET}	1442 [kJ/s]
$ExdestRC_{LPT}$	301.2 [kJ/s]	W_{PUMP}	35.4 [kJ/s]
$ExdestRC_{PUMP}$	28.09 [kJ/s]	WRC_{HPT}	803.8 [kJ/s]
Exq_{ABS}	20.44 [kJ/s]	WRC_{LPT}	639 [kJ/s]
Exq_{CHX}	-8.979 [kJ/s]	WRCpump	0.8901 [kJ/s]]
Exq_{CON}	7.07 [kJ/s]	W_{TOTAL}	1443 [kJ/s]
Exq_{EVA}	-27.51 [kJ/s]	UF	17.65%
Exq_{HHX}	0.6068 [kJ/s]		

4.1 Effect of Evaporator Mass Flow rate on the Energetic and Exergetic COPs

As it is shown in Figure 4.1, by increasing the evaporator mass flow rate of the system, both energetic and exergetic COPs are increasing due to raise in the evaporator heat transfer rate and increase in the work produced by the DEACS. By cosidering the folowing figure, by increasing the evaporator mass flow rate from 0.167 kg/s to 1kg/s, both energetic and egergetic COPs are increasing from 1.437to 8.605 and 0.3371 to 2.018, respectively. It is noticable that energetic line trend goes higher than the exergetic one due to the losses (exergy destruction) of the system in

exergetic analysis (exergetic reluts are less than energetic results in all the system simulation because of the irriversibilities).

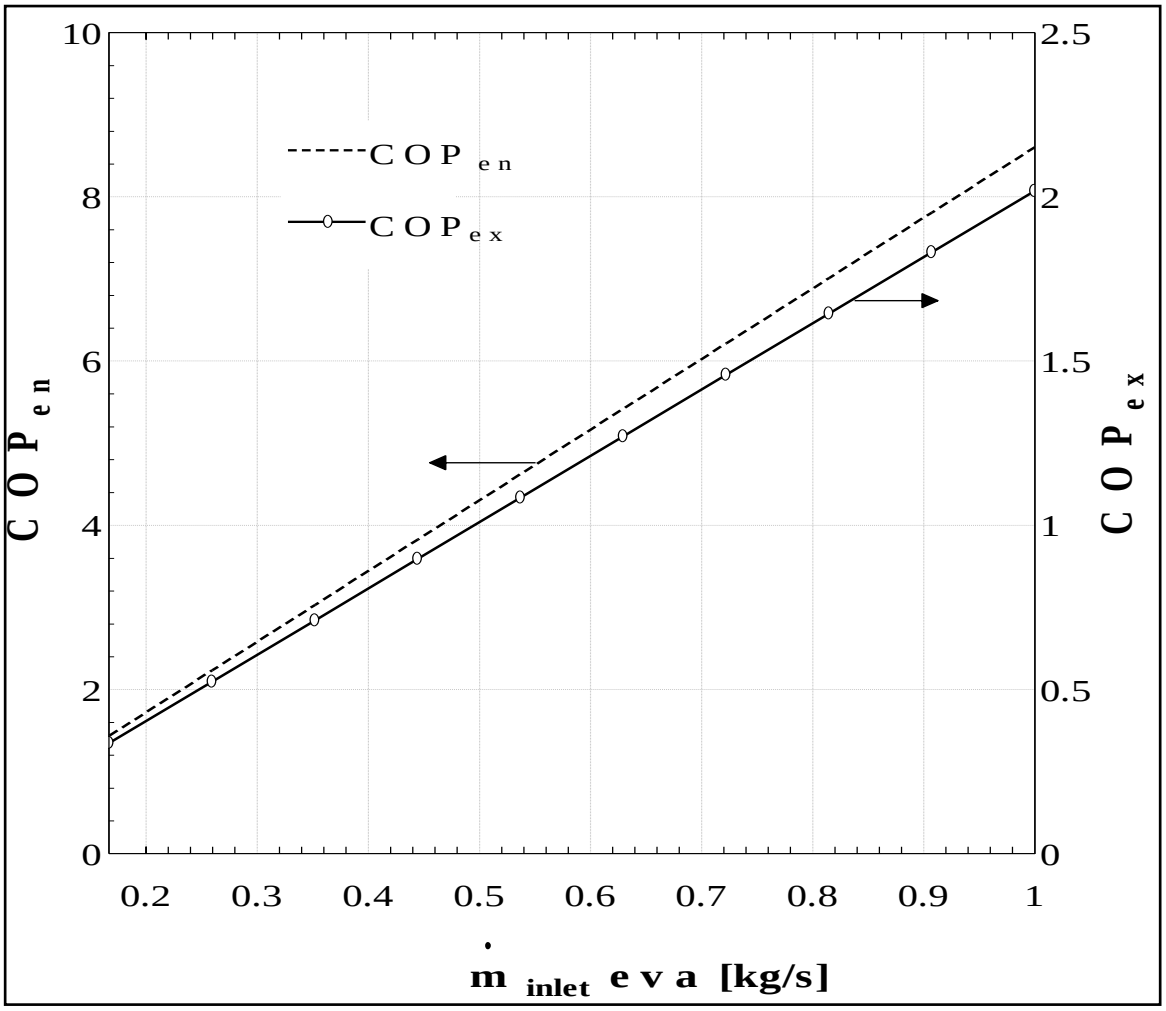

Figure 4.1: Effects of evaporator mass flow on the energetic and exergetic COPs

4.2 Ambient temperature effects on the energetic and exergetic COPs

Figure 4.2 shows the effect of ambient temperature on the performance of DEACS.By increasing the environment temperature of the system, from 22 °C to 47°C, the COP exergy increases from 0.27 to 0.9. This is expected to the reduction in the temperature difference between the reference ambient temperture and the cooling system. On the other hand there is not any change in energetic COP because it is autonomous from the environment temperarture.

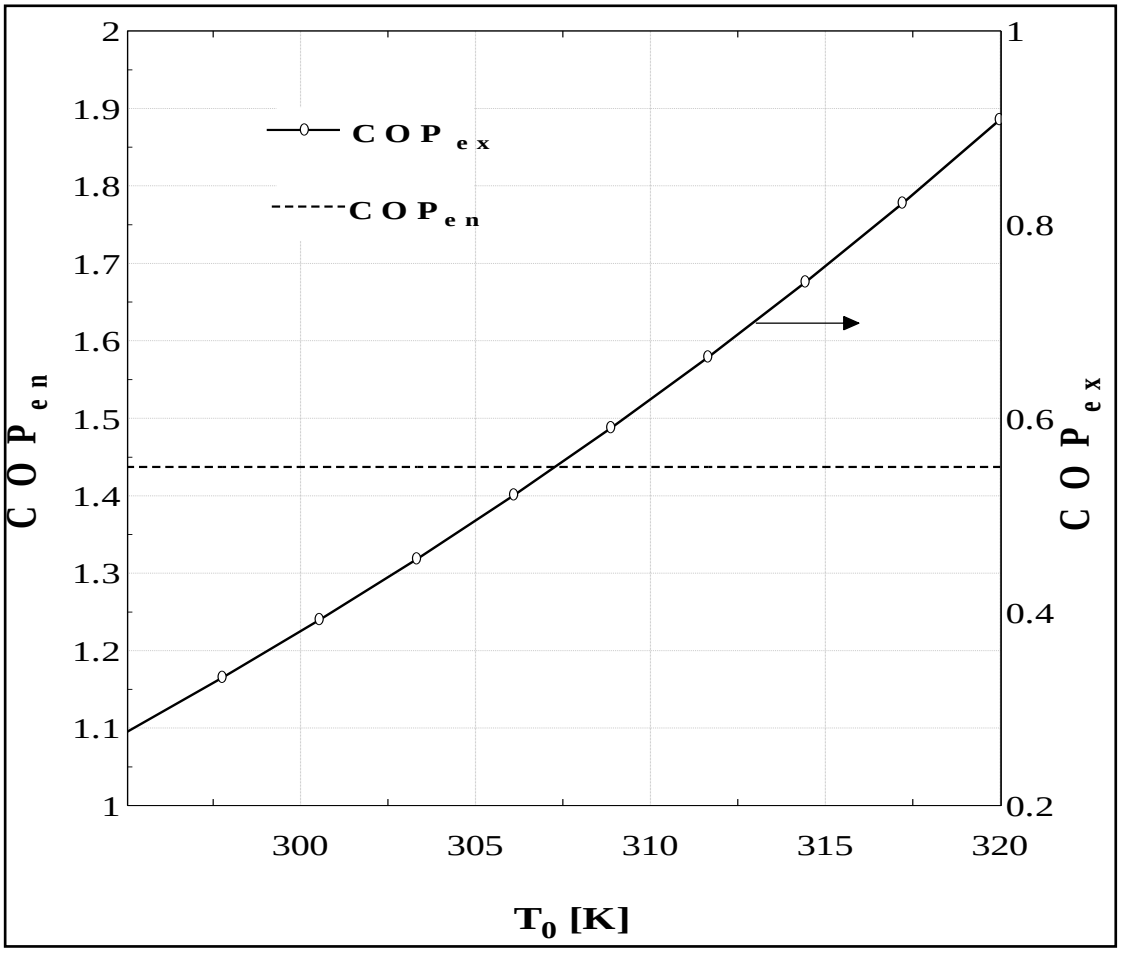

Figure 4.2: Ambient temperature effects on the energetic and exergetic COPs

4.3 Effect of Rankine Cycle Mass Flow Rate on the Energetic and Exergetic Efficiency

As it is shown in Figure 4.3, by increasing inlet Rankine cycle mass flow rate from 1 kg/s to 10 kg/s, both energetic and egergetic efficiency are increasing from 1.4% to 14.08% and 1.7% to 18.01 %, respectively. It is noticable that energetic line trend goes higher than the exergetic one due to the losses of the system in exergetic analysis (exergetic reluts are less than energetic results in all the system simulation because of considering the irriversibility).

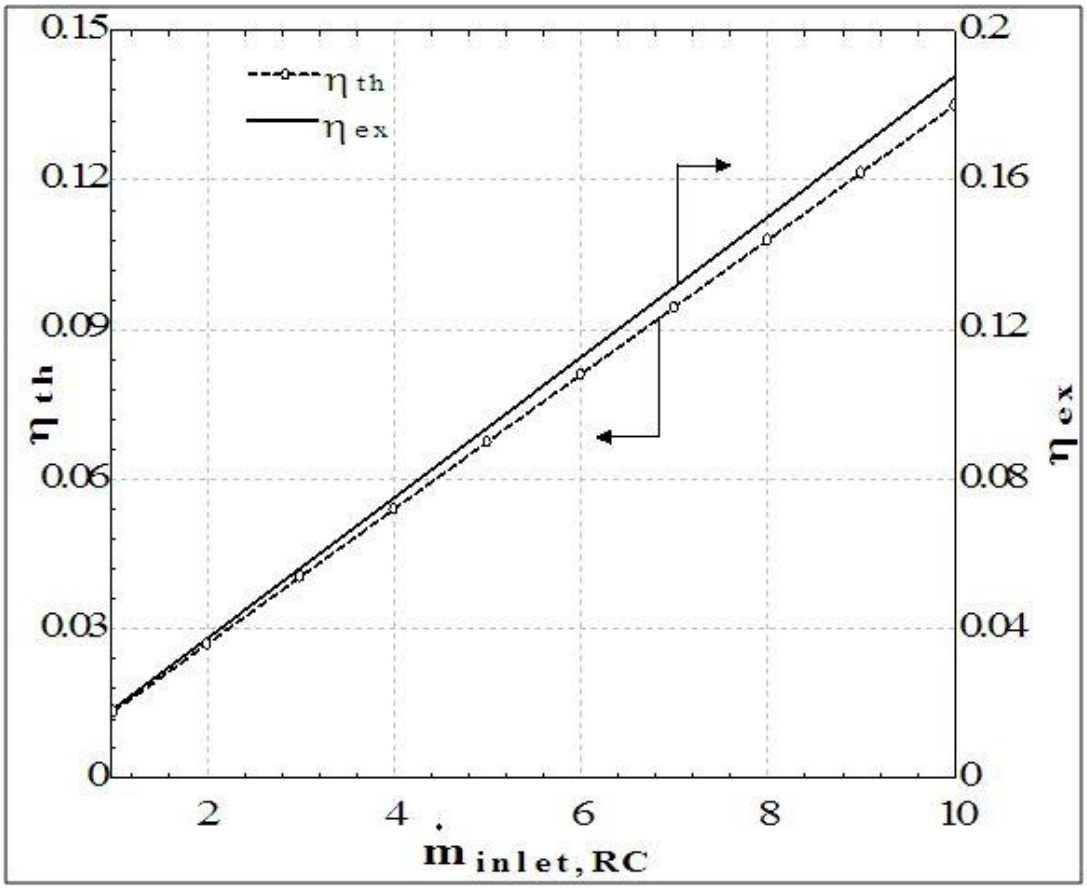

Figure 4.3: Effect of inlet mass flow rate of Ranking Cycle on the energetic and exergetic efficiency

4.4 Effect of variation in the High Temperature Generator on the Energetic and Exergetic COPs

As it is shown in Figure 4.4, by increasingheat input to the high pressure temperture generater of the system from 200 kJ/s to 500kJ/s, both energetic and egergetic COPs are deccreasing from 1.766 to 0.7762 and 0.3831 to 0.2176, respectively,and decreasing of COPs is due to raise the the amount of heat HTG which higher than heat enhancement inthe evaporator

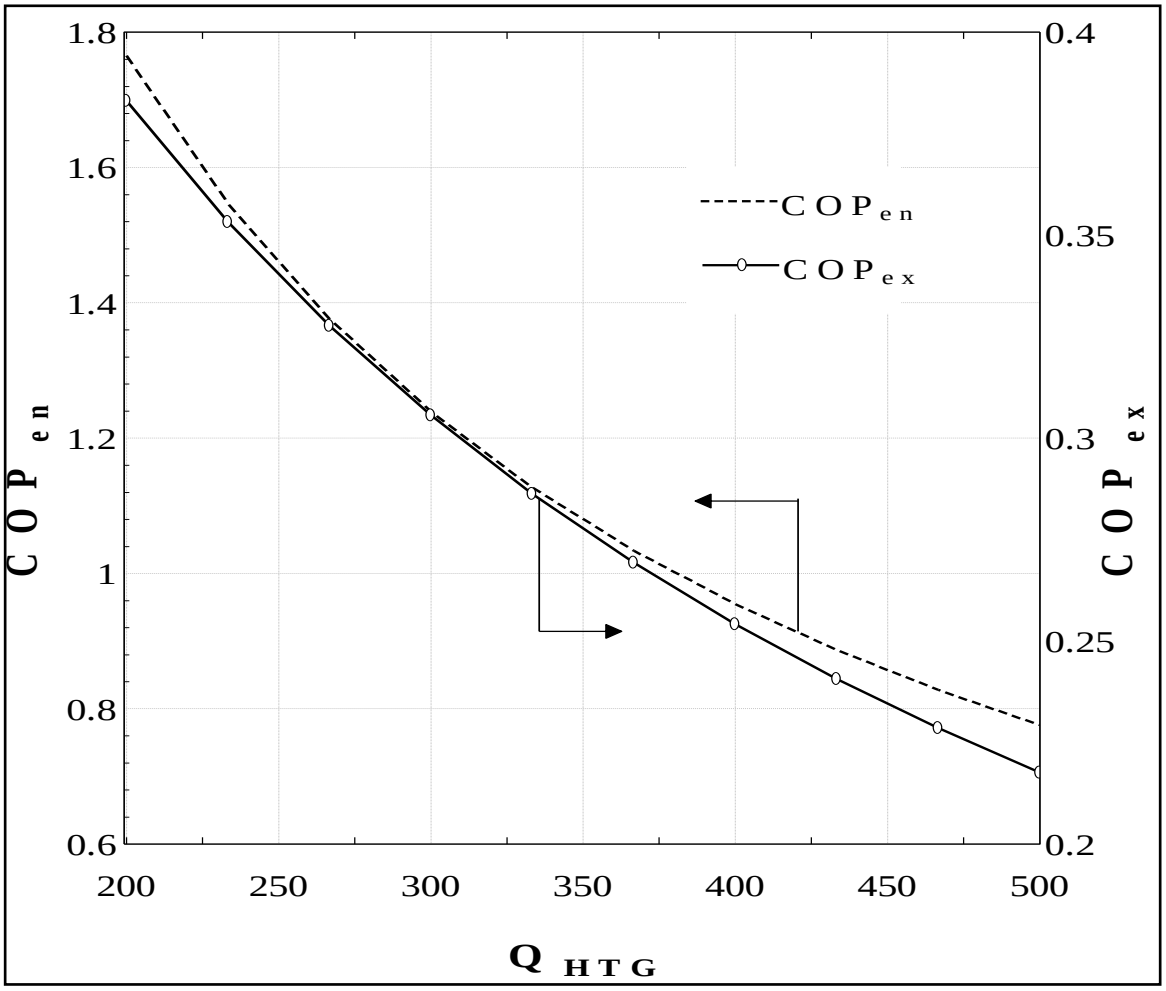

Figure 4.4: Variation in the heat transfer rate effect of HTG on the energetic and exergetic COPs

4.5 Effect of Evaporator Heat on the Energetic and Exergetic COPs

As it is shown in Figure 4.5, by incresing the heat flow rate of evaporator from 200 kJ/s to 500 kJ/s, energetic and egergetic COP_s are increasing from 0.6916 to 1.729 and 0.1622 to 0.4055, respectively.It is noticable that energetic line trend goes higher than the exergetic one due to considering the losses of the system in exergetic analysis.

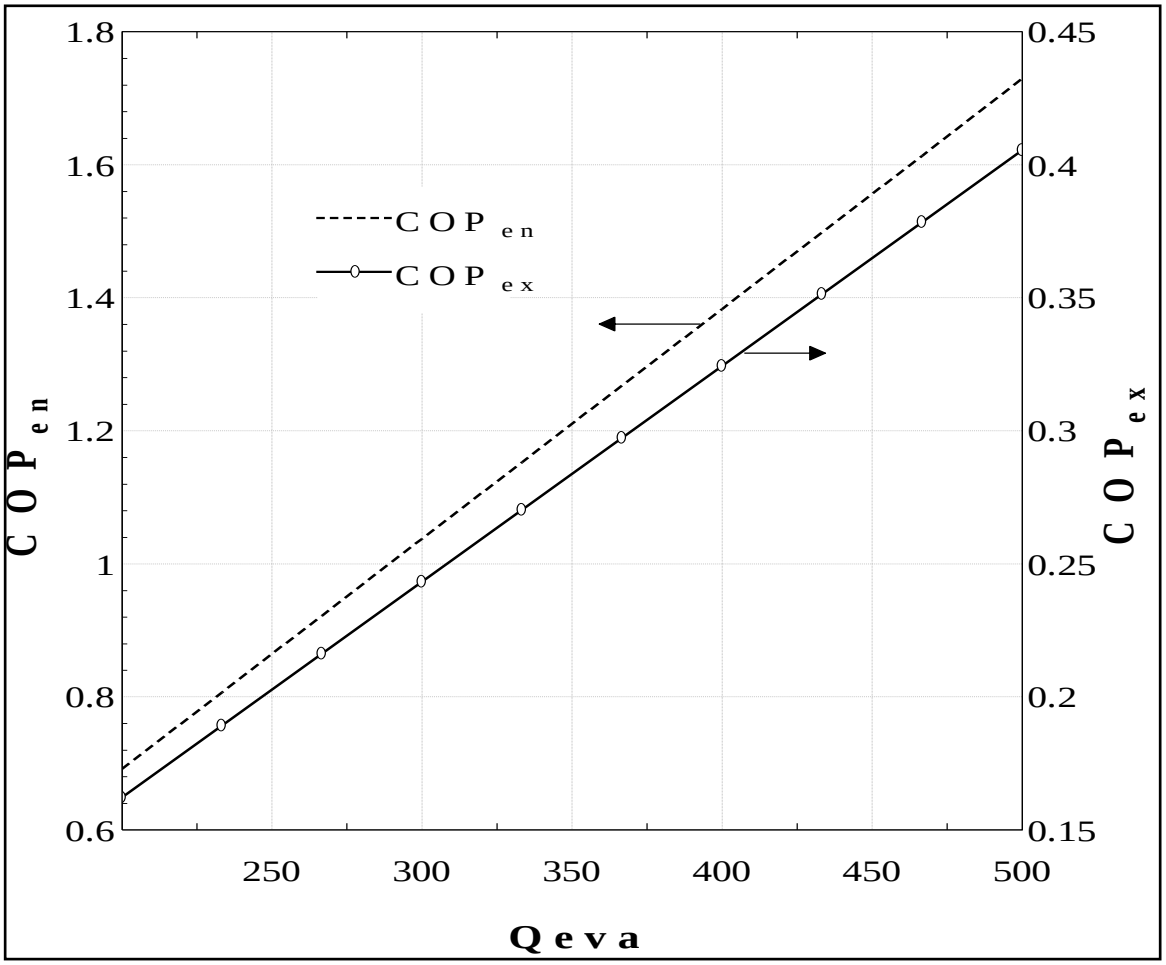

Figure 4.5: Variation in the heat transfer rate effect of evaporator on the energetic and exergetic COPs

4.6 The Environment Temperature Effects on the Energetic and Exergetic Efficiencies

Figure 6 shows the effect of ambient temperature on the performance of Rankine Cycle. By increasing the environment temperature of the system,from 17°C to 47°C, exergetic efficiency is abit increasing from 16.14% to 16.37%.This is result of reducing in system and the temperature difference between the reference ambint . On the other hand there is not any change on energetic efficiency because it is independent from the environment temperarture

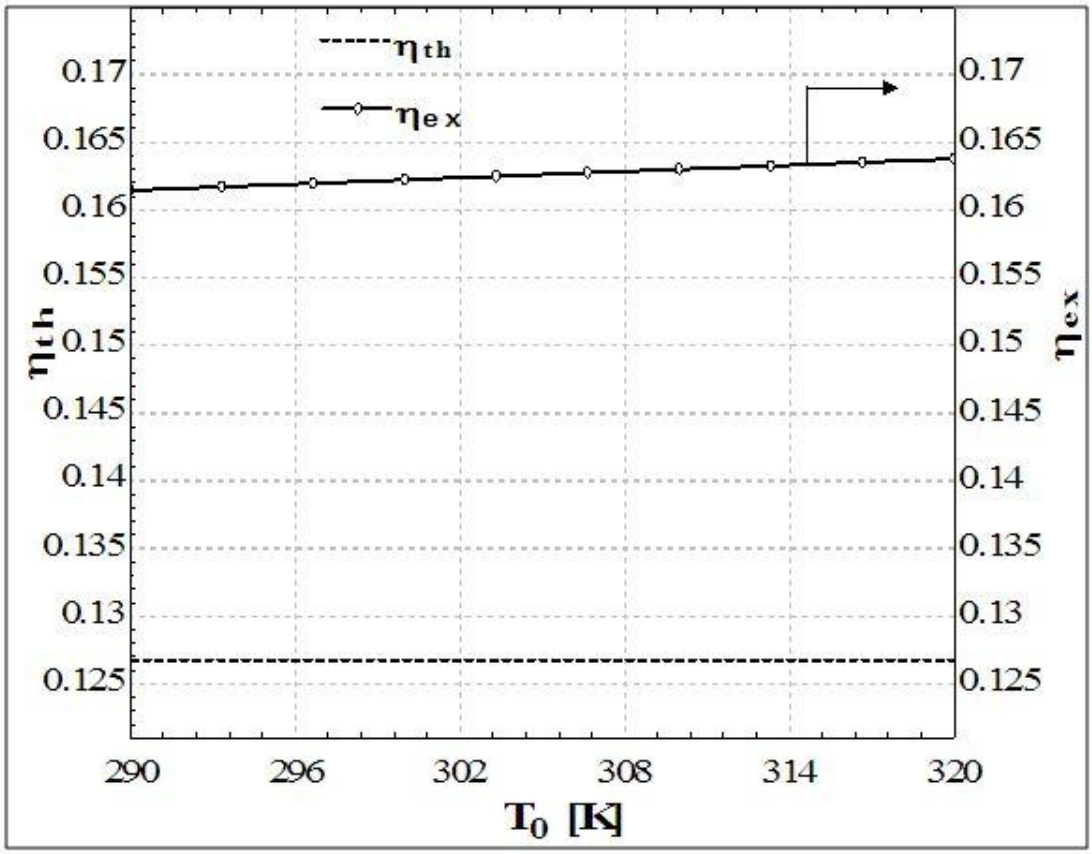

Figure 4.6: Effects of environment temperature on the energetic and exergetic efficiency

4.7 Effect of Inlet Pressure Turbine on the Energy and Exergy Efficiency

As it is shown in Figure 4.7, by In decreasing in let pressure of turbine of the system from 900 kPa to 200 kPa, both energetic and egergetic efficincy are increasing from 12.67% to 16.35 % and 16.21% to 20.91%, respectively,It is noticable that energetic line trend gose higher than the exergetic one due to considering the losses of the system in exergetic analysis

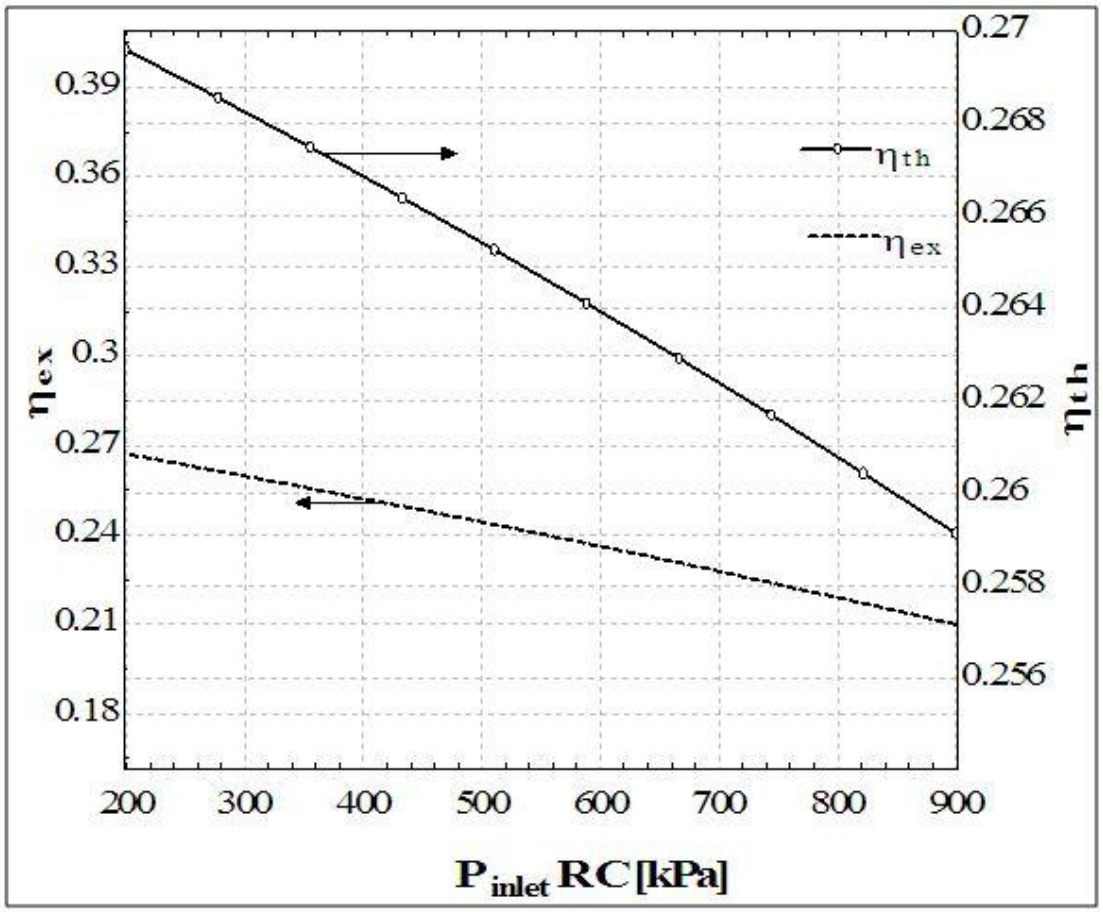

Figure 4.7: Effect of Inlet pressure turbine on the energetic and exergetic efficiency

4.8 Effect of Rankine Cycle Mass Flow Rate on the High and Low Pressure Turbines

As it is shown in Figure 4.8, by increasing the inlet Ranking cycle mass flow rate mass flow rate of the system from 9 kg/s to 20 kg/s, both low pressure turbine and high pressure turbine producing work are increasing from 639 kJ/s to 1420 kJ/s and 803.8 kJ/s to 1786 kJ/s, respectively.

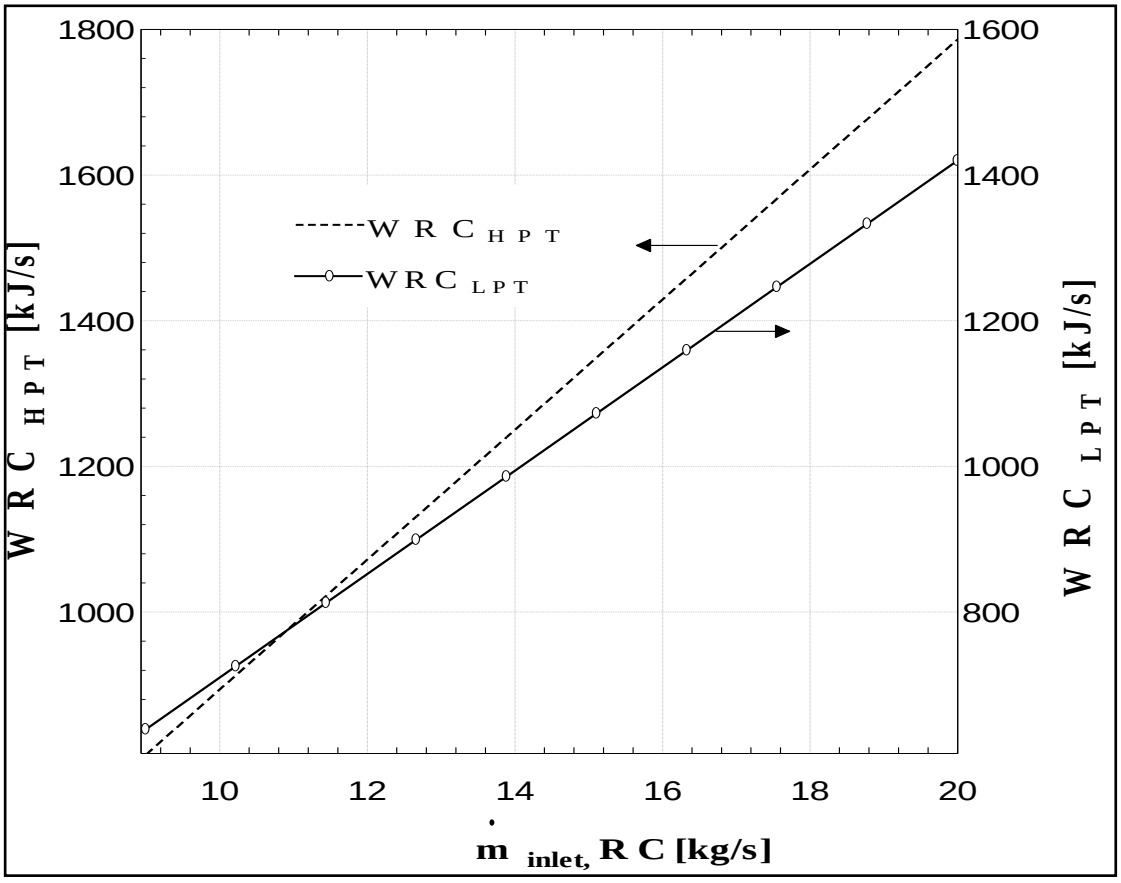

Figure 4.8: Effects of mass flow rate Rankine Cycle on the high and low pressure turbines

4.9 The evaporator inlet temperature effects on the Energy and Exergy COPs and Evaporator Heat Transfer Rate

The Figure 4.9 presents the effect of inlet evaporator temperature on the performance of DEACS and heat flow rate in evaporator. By increasing the inlet evaporator temperature of the system,from 1 °C to 6°C, both energetic and egergetic COP_s are decreasing from 1.449 to 1.437 and 0.3894 to 0.3371, respectively also evaporator heat decreasing from 419.1 kJ/sto 415.6 kJ/s.

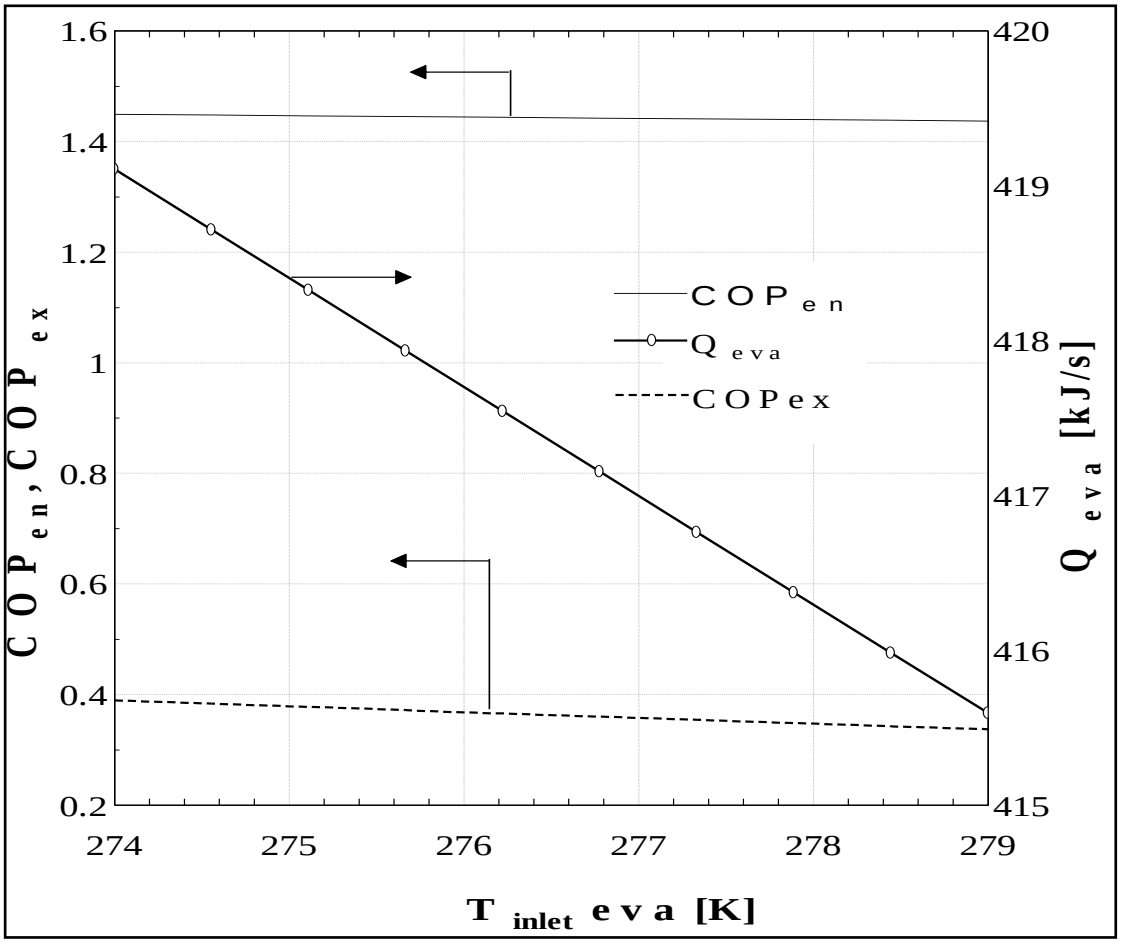

Figure 4.9: Effect of Inlet evaporator temperature on the energetic and exergetic COPs and evaporator heat

4.10 Effect of Net Work on the Mass Produces of Hydrogen and Utilization Factor

As it is shown in Figure 4.10, by increasing the work net of the cycle 500 kW to 3500 kW, both mass of hydrogen production and utilization factor are increasing from 0.000776 kg/s to 0.00543 kg/s and 9.372% to 35.74%, respectively,whears the heat

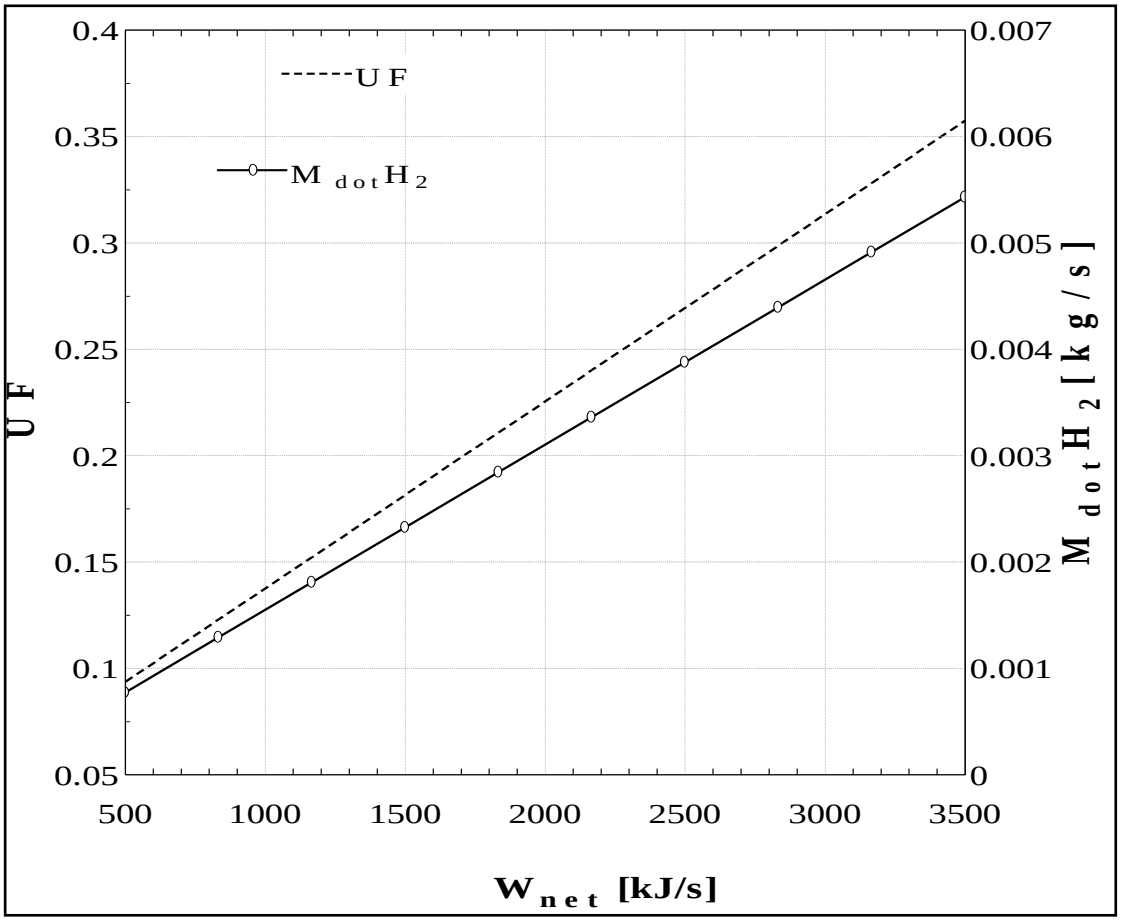

Figure 4.10: Effect of net work on the mass produces of hydrogen and utilization factor

4.11 Exergy Destruction Rates for Components

As it is shown in Figure 4.11, the exergy destruction analysis show up that the system components have a large number of exergy destruction is high pressure turbine(the destruction rate becomes maximum). Both low and high pressure turbines has destruction rate more than 4000 kW that can be reduced by implementing suitable assumptions, temperature and pressure parameters. On the other hand pump and condenser includes all the less amount of exergy destruction and this accounts for the negligence of the heat lost in the system .

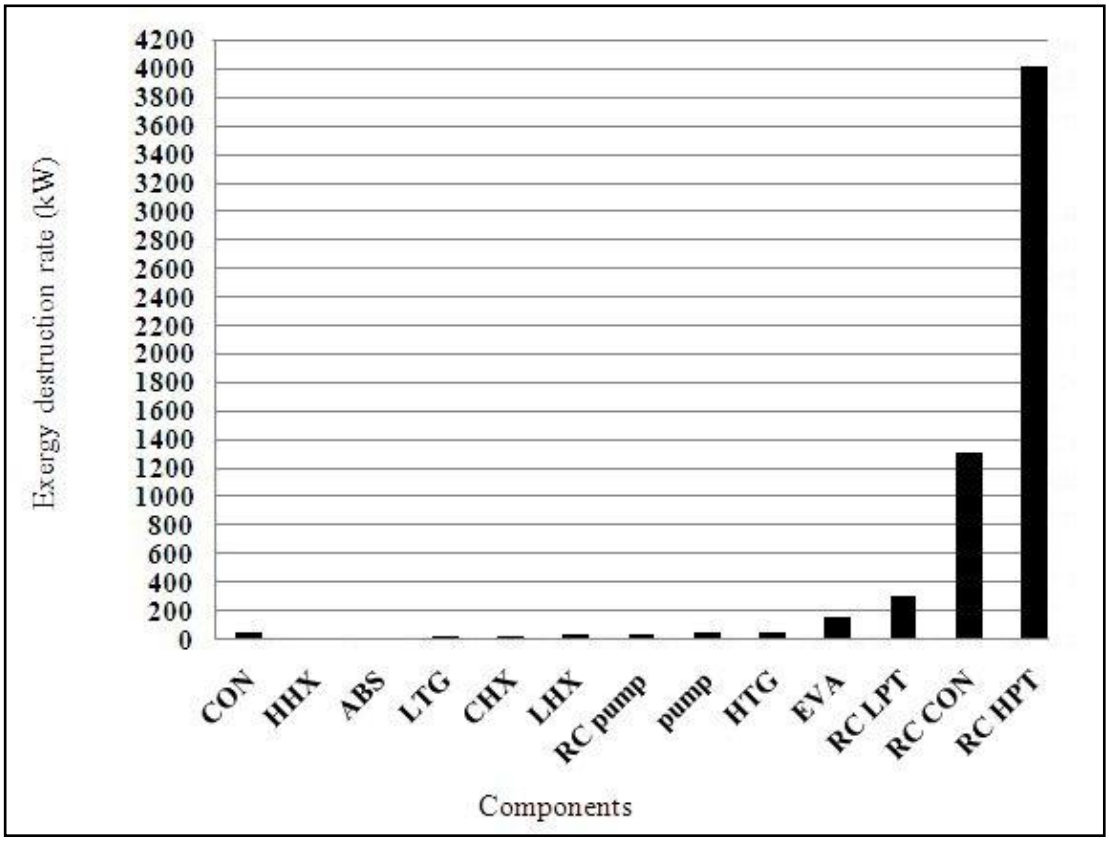

Figure 4.11: Exergy destruction rates for different components

Chapter 5

CONCLUSIONS AND FUTURE WORK

This study, investigates a renewable energy based multigeneration system which uses geothermal energy to meet the energy requirements of building. The multigeneration system is proposed for electricity generation, cooling, and hot water generation. It is also aimed to produce hydrogen. The main reason that led to this study is to increase efficiency and reduce environmental impacts of separate production.

The electricity production is achieved by geothermal based Rankine cycle. The cooling on the other hand is supplied by double effect absorption cooling system which is also based on geothermal water. Energy and exergy analysis has been approved for the proposed system by using EES software. By the results reached by the study is very convincing due to the use of geothermal. The subsystems and overall system has been investigated under various operating conditions. A parametric study is conducted to investigate the effect of various parameters such as various mass flow rate, pressure, and ambient temperature on the total efficiencies of the system. The total efficiencies of the system are so sensitive to the increasing of ambient temperature of the system. Variation of exergy efficiency and exergy destruction rate with changing ambient temperature, with varying ambient temperature of geothermal exergy destruction rate and exergy efficiency, variation of energetic and exergetic COPs with changing inlet mass flow rate of evaporator. Variation of energetic and exegetic efficiency with changing inlet mass flow rate of

Rankine cycle , variation of energetic and exegetic efficiency with changing inlet pressure and temperature of Rankine cycle, and variation of energetic and exergetic COPs with changing heat high temperature generator and heat of evaporator, has been investigated.

After the system design process and, data entry to the Software EES results were obtained. The energy and exergy efficiencies of the Rankine Cycle are found to be 25.91% and 20.99%, respectively, and it has been found that these efficiencies increase by increasing inlet mass flow rate and pressure.

In this studies Parametric are performed to observe the effects of different parameters namely inlet pressure and temperature of the RC high pressure and low pressure turbines, and reference environment temperature on exergy analysis. The energy and exergy COPs of the double effect absorption cooling system are found to be 1.437 and 0.3371 respectively, and increase in these values by increasing inlet mass flow rate and heat of evaporator has been absorbed. Exergy destruction is calculated for all components, the minimum is in the condenser of DEACS 1.321kW and maximum is in RC high pressure turbine 4021 kW. The overall utilization factor has been found as 17.65 %.

The results which are presented in this thesis should be used to develop or design new multigeneration systems for improving results in future.

From the performed analyses, the following studies should be considered, studying environmental impact and exergy economic parameters of these integrated systems to be able to recognize the effect on the economics of the integrated systems.

REFERENCES

[1] Shortall, R., Davidsdottir, B., & Axelsson, G. (2015). *Development of a sustainability assessment framework for geothermal energy projects*. Energy for Sustainable Development, 27, 28-45.

[2] Wight, N. M., & Bennett, N. S. (2015). *Geothermal energy from abandoned oil and gas wells using water in combination with a closed wellbore.* Applied Thermal Engineering, 89, 908-915.

[3] *Population and Demography Forum*.(2003). Retrieved from http://populationforum.org/yaf_poststst4193_Energy-conversion.aspx

[4] *Cogeneration / Combined Heat and Power (CHP)*. (2011, March). Retrieved from http://www.c2es.org/technology/factsheet/CogenerationCHP

[5] Dincer, I., & Rosen, M. A. (2012). *Exergy: energy, environment and sustainable development.* Newnes.

[6] Ahmadi, P. (2013). *Modeling, analysis and optimization of integrated energy systems for multigeneration purposes* (Doctoral dissertation, Faculty of Engineering and Applied Science, University of Ontario Institute of Technology).

[7] Maidment, G. G., & Tozer, R. M. (2002). *Combined cooling heat and power in supermarkets.* Applied thermal engineering, 22(6), 653-665.

[8] Tracy, B. L. (2007). *Visuomotor contribution to force variability in the plantarflexor and dorsiflexor muscles.* Human movement science, 26(6), 796-807.

[9] Huang, F. J., Boureau, Y. L., & LeCun, Y. (2007, June). *Unsupervised learning of invariant feature hierarchies with applications to object recognition.* In 2007 IEEE conference on computer vision and pattern recognition (pp. 1-8). IEEE.

[10] Foster, J. E., Lopez-Calva, L. F., & Szekely, M. (2005). *Measuring the distribution of human development: methodology and an application to Mexico*. Journal of Human Development, 6(1), 5-25.

[11] Ziher, D., & Poredos, A. (2006). *Economics of a trigeneration system in a hospital.* Applied Thermal Engineering, 26(7), 680-687.

[12] Misra, P., Khaliq, T., Dixit, A., SenGupta, S., Samant, M., Kumari, S, & Narender, T. (2008*). Antileishmanial activity mediated by apoptosis and structure-based target study of peganine hydrochloride dihydrate: an approach for rational drug design.* Journal of antimicrobial chemotherapy, 62(5), 998-1002.

[13] Beberg, A. L., Ensign, D. L., Jayachandran, G., Khaliq, S., & Pande, V. S. (2009, May). Folding@ home: *Lessons from eight years of volunteer distributed computing.* In Parallel & Distributed Processing, 2009. IPDPS 2009. IEEE International Symposium on (pp. 1-8). IEEE.

[14] Jääskeläinen, H. E., & Wallace, J. S. (2009, January). *Thermal Performance of a Combined Heat, Cooling, and Power Microturbine System.* In ASME 2009 3rd International Conference on Energy Sustainability collocated with the Heat Transfer and InterPACK09 Conferences (pp. 209-219). American Society of Mechanical Engineers.

[15] Flexas, J., Bota, J., Galmes, J., Medrano, H., & Ribas-Carbó, M. (2006). *Keeping a positive carbon balance under adverse conditions: responses of photosynthesis and respiration to water stress*. Physiologia Plantarum, 127(3), 343-352.

[16] Yu, M. L., Dai, C. Y., Huang, J. F., Hou, N. J., Lee, L. P., Hsieh, M. Y., ... & Wang, L. Y. (2007). *A randomised study of peginterferon and ribavirin for 16 versus 24 weeks in patients with genotype 2 chronic hepatitis C.* Gut, 56(4), 553-559.

[17] Fredman, P., & Tyrväinen, L. (2010). *Frontiers in nature-based tourism.* Scandinavian Journal of Hospitality and Tourism, 10(3), 177-189.

[18] Flexas, J., Ribas-Carbo, M. I. Q. U. E. L., DIAZ-ESPEJO, A. N. T. O. N. I. O., GalmES, J., & Medrano, H. (2008). Mesophyll conductance to CO2: *current knowledge and future prospects*. Plant, Cell & Environment, 31(5), 602-621.

[19] Cho, K., Van Merriënboer, B., Bahdanau, D., & Bengio, Y. (2014). *On the properties of neural machine translation*: Encoder-decoder approaches. arXiv preprint arXiv:1409.1259.

[20] Al-Sulaiman, F. A., Hamdullahpur, F., & Dincer, I. (2011). *Trigeneration: a comprehensive review based on prime movers.* International journal of energy research, 35(3), 233-258.

[21] Rosiek, S., & Batlles, F. J. (2013). *Renewable energy solutions for building cooling, heating and power system installed in an institutional building: Case study in southern Spain.* Renewable and Sustainable Energy Reviews, 26, 147-168.

[22] Wang, Y., Leung, H. C., Yiu, S. M., & Chin, F. Y. (2012). MetaCluster 5.0: *a two-round binning approach for metagenomic data for low-abundance species in a noisy sample.* Bioinformatics, 28(18), i356-i362.

[23] Atwell, S., Huang, Y. S., Vilhjálmsson, B. J., Willems, G., Horton, M., Li, Y., ... & Jiang, R. (2010). *Genome-wide association study of 107 phenotypes in Arabidopsis thaliana inbred lines.* Nature, 465(7298), 627-631.

[24] Ozcan, H., & Dincer, I. (2013). *Thermodynamic analysis of an integrated sofc, solar orc and absorption chiller for tri-generation applications.* Fuel Cells, 13(5), 781-793.

[25] Babu, B. J., Maldonado, A., Velumani, S., & Asomoza, R. (2010). *Electrical and optical properties of ultrasonically sprayed Al-doped zinc oxide thin films.* Materials Science and Engineering: B, 174(1), 31-37.

[26] Jones, E. V., Bernardinelli, Y., Tse, Y. C., Chierzi, S., Wong, T. P., & Murai, K. K. (2011). *Astrocytes control glutamate receptor levels at developing synapses through SPARC–β-integrin interactions.* The Journal of Neuroscience, 31(11), 4154-4165.

[27] Kocher, A. A., Schuster, M. D., Szabolcs, M. J., Takuma, S., Burkhoff, D., Wang, J & Itescu, S. (2001). *Neovascularization of ischemic myocardium by human bone-marrow–derived angioblasts prevents cardiomyocyte apoptosis, reduces remodeling and improves cardiac function.* Nature medicine, 7(4), 430-436.

[28] Cohce, M. K., Dincer, I., & Rosen, M. A. (2011). *Energy and exergy analyses of a biomass-based hydrogen production system.* Bioresource technology, 102(18), 8466-8474.

[29] Cengel, Y., & Boles, M. (2014). *Loose leaf for thermodynamics: An engineering approach*. McGraw-Hill Education.

APPENDIX

Engineering Equation Solver Software Codes

```
"Double Effect Absorption Cooling System"

t[0]=298
h[0]=Enthalpy(Air,T=T[0])
p[0]=101
s[0]=Entropy(Air,T=T[0],P=P[0])

"Pump"

t[1]=303.5
p[1]=0.86
m_dot[1]=0.5
x[1]=x_LiBrH2O(T[1],P[1])
h[1]=h_LiBrH2O(T[1],x[1])
s[1]=s_LiBrH2O(T[1],x[1])
ex[1]=(h[1]-h[0])-t[0]*(s[1]-s[0])

p[2]=8.4
t[2]=303.8
m_dot[2]=0.5
h[2]=h_LiBrH2O(T[2],x[2])
x[2]=x_LiBrH2O(T[2],P[2])
s[2]=s_LiBrH2O(T[2],x[2])
ex[2]=(h[2]-h[0])-t[0]*(s[2]-s[0])

WPUMP=m_dot[1]*(h[2]-h[1])/0.85
exdpump=m_dot[1]*ex[1]-m_dot[2]*ex[2]+WPUMP

"Low Temp. Heat Exchanger"
p[3]=8.4
t[3]=320
h[3]=h_LiBrH2O(T[3],x[3])
x[3]=x_LiBrH2O(T[3],P[3])
m_dot[3]=0.4
s[3]=s_LiBrH2O(T[3],x[3])
ex[3]=(h[3]-h[0])-t[0]*(s[3]-s[0])

t[14]=319
p[14]=8.4
s[14]=s_LiBrH2O(T[14],x[14])
m_dot[14]=0.3331
h[14]=h_LiBrH2O(T[14],x[14])
x[14]=x_LiBrH2O(T[14],P[14])
ex[14]=(h[14]-h[0])-t[0]*(s[14]-s[0])

t[15]=280
p[15]=8.4
s[15]=s_LiBrH2O(T[15],x[15])
m_dot[15]=m_dot[14]
h[15]=h_LiBrH2O(T[15],x[15])
x[15]=x_LiBrH2O(T[15],P[15])
ex[15]=(h[15]-h[0])-t[0]*(s[15]-s[0]
```

```
t[19]=355
p[19]=8.4
s[19]=s_LiBrH2O(T[19],x[19])
x[19]=x_LiBrH2O(T[19],P[19])
h[19]=h_LiBrH2O(T[19],x[19])
m_dot[19]=m_dot[3]
ex[19]=(h[19]-h[0])-t[0]*(s[19]-s[0])

QLHE=m_dot[3]*h[3]-m_dot[19]*h[19]
exqLHE=(1-t[0]/(t[19]/2+t[3]/2))*QLHE
exdLHE=m_dot[19]*ex[19]-m_dot[3]*ex[3]+exqLHE

"High Temp. Heat Exchanger"

p[20]=8.4
x[20]=x_LiBrH2O(T[20],P[20])
t[20]=333
h[20]=h_LiBrH2O(T[20],x[20])
s[20]=s_LiBrH2O(T[20],x[20])
m_dot[20]=m_dot[4]
ex[20]=(h[20]-h[0])-t[0]*(s[20]-s[0])

t[12]=353
p[12]=8.4
h[12]=h_LiBrH2O(T[12],x[12])
s[12]=s_LiBrH2O(T[12],x[12])
x[12]=x_LiBrH2O(T[12],P[12])
m_dot[12]=0.2132
ex[12]=(h[12]-h[0])-t[0]*(s[12]-s[0])

t[13]=347
p[13]=8.4
x[13]=x_LiBrH2O(T[13],P[13])
s[13]=s_LiBrH2O(T[13],x[13])
h[13]=h_LiBrH2O(T[13],x[13])
m_dot[13]=m_dot[12]
ex[13]=(h[13]-h[0])-t[0]*(s[13]-s[0])

t[4]=365
h[4]=h_LiBrH2O(T[4],x[4])
x[4]=x_LiBrH2O(T[4],P[4])
p[4]=8.4
s[4]=s_LiBrH2O(T[4],x[4])
m_dot[4]=0.32
ex[4]=(h[4]-h[0])-t[0]*(s[4]-s[0])

QHHE=m_dot[12]*h[12]-m_dot[13]*h[13]
exqHHE=(1-t[0]/(t[12]/2+t[13]/2))* QHHE
exdHHE=m_dot[12]*ex[12]-m_dot[13]*ex[13]+exqHHE
```

```
" High Tem.Generator"

t[5]=375
p[5]=8.4
h[5]=Enthalpy(Water,T=T[5],P=P[5])
s[5]=Entropy(Water,T=T[5],P=P[5])
m_dot[5]=0.1069
ex[5]=(h[5]-h[0])-t[0]*(s[5]-s[0])
QHTG=(m_dot[5]*h[5])+(m_dot[12]*h[12])-(m_dot[4]*h[4])
exqHTG=(1-t[0]/(t[12]/3+t[5]/3+t[4]/3))*QHTG
exdHTG=m_dot[4]*ex[4]-m_dot[5]*ex[5]-m_dot[12]*ex[12]+exqHTG

"Low Temp.Generator"

t[22]=365
p[22]=8.4
x[22]=x_LiBrH2O(T[22],P[22])
h[22]=h_LiBrH2O(T[22],x[22])
s[22]=s_LiBrH2O(T[22],x[22])
m_dot[22]=0.18

t[6]=317
h[6]=Enthalpy(Water,T=T[6],P=P[6])
p[6]=8.4
s[6]=Entropy(Water,T=T[6],P=P[6])
m_dot[6]=m_dot[5]
ex[6]=(h[6]-h[0])-t[0]*(s[6]-s[0])

h[23]=h_LiBrH2O(T[23],x[23])
t[23]=302
p[23]=8.4
x[23]=x_LiBrH2O(T[23],P[23])
s[23]=s_LiBrH2O(T[23],x[23])
m_dot[23]=0.1199

t[7]=338
h[7]=Enthalpy(Water,T=T[7],P=P[7])
p[7]=8.4
s[7]=Entropy(Water,T=T[7],P=P[7])
ex[7]=(h[7]-h[0])-t[0]*(s[7]-s[0])
m_dot[7]=0.0601

QLTG=(m_dot[23]*h[23])+(m_dot[6]*h[6])+(m_dot[7]*h[7])-(m_dot[22]
*h[22])-(m_dot[5]*h[5])
exqLTG=(1-t[0]/(t[23]/5+t[7]/5+t[22]/5+t[6]/5+t[5]/5))* QLTG
exdLTG=-m_dot[6]*ex[6]-m_dot[23]*ex[23]-m_dot[7]*ex[7]+m_dot[22]*
ex[22]+m_dot[5]*ex[5]+exqLTG

ex[22]=(h[22]-h[0])-t[0]*(s[22]-s[0])
ex[23]=(h[23]-h[0])-t[0]*(s[23]-s[0])
"Condenser Heat Exchanger"
```

```
t[17]=323
p[17]=8.4
m_dot[17]=0.1
h[17]=h_LiBrH2O(T[17],x[17])
x[17]=x_LiBrH2O(T[17],P[17])
s[17]=s_LiBrH2O(T[17],x[17])
ex[17]=(h[17]-h[0])-t[0]*(s[17]-s[0])

t[18]=313
p[18]=8.4
h[18]=h_LiBrH2O(T[18],x[18])
x[18]=x_LiBrH2O(T[18],P[18])
s[18]=s_LiBrH2O(T[18],x[18])
m_dot[18]=m_dot[17]
ex[18]=(h[18]-h[0])-t[0]*(s[18]-s[0])

QCHE=-m_dot[6]*h[6]+m_dot[8]*h[8]
exqCHE=(1-t[0]/(t[8]/2+t[6]/2))* QCHE
exdCHE=m_dot[6]*ex[6]-m_dot[8]*ex[8]-exqCHE

" Condenser"

t[8]=300
p[8]=8.4
h[8]=Enthalpy(Water,T=T[8],P=P[8])
s[8]=Entropy(Water,T=T[8],P=P[8])
m_dot[8]=0.1069
ex[8]=(h[8]-h[0])-t[0]*(s[8]-s[0])

t[9]=t[8]
p[9]=8.4
h[9]=Enthalpy(Water,T=T[9],P=P[9])
m_dot[9]=0.167
s[9]=Entropy(Water,T=T[9],P=P[9])

QCOND=m_dot[7]*h[7]+m_dot[8]*h[8]-m_dot[9]*h[9]
ex[9]=(h[9]-h[0])-t[0]*(s[9]-s[0])
exqCOND=(1-t[0]/(t[8]/3+t[7]/3+t[9]/3))*QCOND
exdCOND=m_dot[7]*ex[7]+m_dot[8]*ex[8]-m_dot[9]*ex[9]-exqCOND

"Evaporator"
t[10]=279
h[10]=Enthalpy(Water,T=T[10],P=P[10])
m_dot[10]=0.167
p[10]=0.95
s[10]=Entropy(Water,T=T[10],P=P[10])
ex[10]=(h[10]-h[0])-t[0]*(s[10]-s[0])

t[11]=280
h[11]=Enthalpy(Water,T=T[11],P=P[11])
```

```
p[11]=0.86
s[11]=Entropy(Water,T=T[11],P=P[11])
ex[11]=(h[11]-h[0])-t[0]*(s[11]-s[0])

QEVAP=m_dot[11]*h[11]-m_dot[10]*h[10]
exqEVAP=(1-t[0]/(t[11]/2+t[10]/2))* QEVAP
exdEVAP=ex[10]-ex[11]+exqEVAP

"Absorber"

p[16]=0.86
t[16]=350
x[16]=x_LiBrH2O(T[16],P[16])
s[16]=s_LiBrH2O(T[16],x[16])
m_dot[16]=m_dot[15]
h[16]=h_LiBrH2O(T[16],x[16])
ex[16]=(h[16]-h[0])-t[0]*(s[16]-s[0])

QABS=m_dot[11]*h[11]+m_dot[16]*h[16]-m_dot[1]*h[1]
exqABS=(1-t[0]/(t[1]/3+t[16]/3+t[11]/3))* QABS
exdABS=m_dot[11]*ex[11]+m_dot[16]*ex[16]-m_dot[1]*ex[1]-exqABS


t[21]=332
p[21]=8.4
x[21]=x_LiBrH2O(T[21],P[21])
s[21]=s_LiBrH2O(T[21],x[21])
h[21]=h_LiBrH2O(T[21],x[21])
m_dot[21]=0.08
ex[21]=(h[21]-h[0])-t[0]*(s[21]-s[0])



t[24]=205+273
p[24]=900
h[24]=Enthalpy(Water,T=T[24],P=P[24])
s[24]=Entropy(Water,T=T[24],P=P[24])
ex[24]=(h[24]-h[0])-t[0]*(s[24]-s[0])
m_dot[24]=3

t[25]=75+273
p[25]=p[24]
h[25]=Enthalpy(Water,T=T[25],P=P[25])
s[25]=Entropy(Water,T=T[25],P=P[25])
ex[25]=(h[25]-h[0])-t[0]*(s[25]-s[0])
m_dot[25]=m_dot[24]



"total COP"

copEn=QEVAP/(wPUMP+QHTG)
```

```
copEx=-exqEVAP/(wPUMP+exqHTG)

"RC High pressure Turbine"

p[29]=900
h[29]=Enthalpy(Water,T=T[29],P=P[29])
s[29]=Entropy(Water,T=T[29],P=P[29])
m_dot[29]=9
ex[29]=(h[29]-h[0])-t[0]*(s[29]-s[0])
t[29]=176+273

p[30]=20
t[30]=100+273
h[30]=Enthalpy(Water,T=T[30],P=P[30])
s[30]=Entropy(Water,T=T[30],P=P[30])
m_dot[30]=m_dot[29]
ex[30]=(h[30]-h[0])-t[0]*(s[30]-s[0])
WRCHT=((m_dot[29]*h[29])-(m_dot[30]*h[30]))
exdRCHT=m_dot[29]*ex[29]-m_dot[30]*ex[30]-WrcHT

"RC Low pressure Turbine"
t[31]=90+273
p[31]=20
h[31]=Enthalpy(Water,T=T[31],P=P[31])
s[31]=Entropy(Water,T=T[31],P=P[31])
m_dot[31]=m_dot[30]
ex[31]=(h[31]-h[0])-t[0]*(s[31]-s[0])

p[32]=10
t[32]=52+273
m_dot[32]=m_dot[31]
h[32]=Enthalpy(Water,T=T[32],P=P[32])
s[32]=Entropy(Water,T=T[32],P=P[32])
ex[32]=(h[32]-h[0])-t[0]*(s[32]-s[0])

WRCLT=((m_dot[31]*h[31])-(m_dot[32]*h[32]))

exdRCLT=m_dot[31]*ex[31]-m_dot[32]*ex[32]-WrcLT
"RC Condencer"
p[33]=10
m_dot[33]=m_dot[32]
x[33]=0
T[33]=Temperature(Acetone,P=P[33],x=x[33])
v[33]=Volume(Water,T=T[33],x=x[33])
h[33]=Enthalpy(Water,P=P[33],x=x[33])
s[33]=Entropy(Water,x=x[33],P=P[33])

ex[33]=(h[33]-h[0])-t[0]*(s[33]-s[0])

QRCcond=m_dot[32]*h[32]-m_dot[33]*h[33]
exqRCcond=(1-t[0]/(t[32]/2+t[33]/2))*qRCcond
exdRCcond=m_dot[32]*ex[32]-m_dot[33]*ex[33]-exqRCcond
```

```
"RC  Pump"

p[34]=900
T[34]=47+273
m_dot[34]=m_dot[33]
h[34]=h[33]+wRCpump
s[34]=Entropy(Water,T=T[34],P=P[34])
ex[34]=(h[34]-h[0])-t[0]*(s[34]-s[0])
WRCpump=v[33]*(p[34]-p[33])
exdRCPump=m_dot[33]*ex[33]-m_dot[34]*ex[34]+WrcPump

"RC Heat Exchanger"
p[27]=900
t[27]=177+273
m_dot[27]=1
h[27]=Enthalpy(Water,T=T[27],P=P[27])
s[27]=Entropy(Water,T=T[27],P=P[27])
ex[27]=(h[27]-h[0])-t[0]*(s[27]-s[0])

p[28]=900
t[28]=110+273
m_dot[28]=m_dot[27]
s[28]=Entropy(Water,T=T[28],P=P[28])
h[28]=Enthalpy(Water,T=T[28],P=P[28])
ex[28]=(h[28]-h[0])-t[0]*(s[28]-s[0])

qRCheatexchanger=-m_dot[31]*h[31]+m_dot[27]*h[27]-m_dot[28]*h[28]
-m_dot[29]*h[29]+m_dot[34]*h[34]+m_dot[30]*h[30]
exqRCheatexchanger=(1-t[0]/(t[27]/6+t[28]/6+t[30]/6+t[29]/6+t[31]
/6+t[34]/6))*qRCheatexchanger
exdRCheatexchanger=-m_dot[31]*ex[31]+m_dot[27]*ex[27]-m_dot[28]*e
x[28]+m_dot[29]*ex[29]-m_dot[34]*ex[34]+m_dot[30]*ex[30]-exqRChea
texchanger

p[26]=900
t[26]=205+273
m_dot[26]=m_dot[27]+m_dot[24]
h[26]=Enthalpy(Water,T=T[26],P=P[26])
s[26]=Entropy(Water,T=T[26],P=P[26])
ex[26]=(h[26]-h[0])-t[0]*(s[26]-s[0])

Wtotal=wrcHT+wrcLT
"Wnet=Wtotal-WRCpump"

EfficiencyTH=Wnet/(m_dot[26]*h[26])

EfficiencyEX=Wnet/(m_dot[26]*ex[26])
```

```
"Electrolyzer"
EFelec=0.55
HHV[1]=141800
m_dotH2=((EFelec*0.4*Wnet)/HHV[1])
MH2=2.016
hH2=4.2004


"Utilization factor"

Uf=(Wnet+QEVAP+QCOND+(m_dotH2*hH2))/(m_dot[26]*h[26])
```